



HAL
open science

Fluid flows and metal deposition near basement/cover unconformity: lessons and analogies from Pb-Zn-F-Ba systems for the understanding of Proterozoic U deposits

M.-C. Boiron, Michel Cathelineau, Antonin Richard

► To cite this version:

M.-C. Boiron, Michel Cathelineau, Antonin Richard. Fluid flows and metal deposition near basement/cover unconformity: lessons and analogies from Pb-Zn-F-Ba systems for the understanding of Proterozoic U deposits. *Geofluids*, 2010, 10, pp.270-292. <10.1111/j.1468-8123.2010.00289.x>. <hal-02437120>

HAL Id: hal-02437120

<https://hal.science/hal-02437120v1>

Submitted on 3 Nov 2024

HAL is a multi-disciplinary open access archive for the deposit and dissemination of scientific research documents, whether they are published or not. The documents may come from teaching and research institutions in France or abroad, or from public or private research centers.

L'archive ouverte pluridisciplinaire **HAL**, est destinée au dépôt et à la diffusion de documents scientifiques de niveau recherche, publiés ou non, émanant des établissements d'enseignement et de recherche français ou étrangers, des laboratoires publics ou privés.



HAL Authorization

**Fluid flows and metal deposition near basement / cover
unconformity: Lessons and analogies from Pb-Zn-F-Ba
systems for the understanding of Proterozoic U deposits**

Journal:	<i>Geofluids</i>
Manuscript ID:	GFL-2009-040.R1
Manuscript Type:	Book Article
Date Submitted by the Author:	
Complete List of Authors:	BOIRON, Marie-Christine; G2R, Nancy Université Cathelineau, Michel; G2R, Nancy Université; CREGU RICHARD, Antonin; G2R, Nancy Université
Key words:	brine, metal, unconformity, extensional tectonic, fluid movement



1
2
3 1
4
5 2
6
7 3 Fluid flows and metal deposition near basement / cover unconformity: Lessons and
8 analogies from Pb-Zn-F-Ba systems for the understanding of Proterozoic U deposits
9 4
10 5
11 6
12 7
13 8
14 9
15 10
16 11
17 12
18 13
19 14
20 15
21 16
22 17
23 18
24 19
25 20
26 21
27 22
28 23
29 24
30 25
31 26
32 27
33 28
34 29
35 30
36 31
37 32
38 33
39 34
40 35
41 36
42 37
43 38
44 39
45 40
46 41
47 42
48 43
49 44
50 45
51 46
52 47
53 48
54 49
55 50
56 51
57 52
58 53
59 54
60 55

Marie-Christine Boiron, Michel Cathelineau and Antonin Richard

G2R, Nancy-Université, CNRS, CREGU, Boulevard des Aiguillettes,
B.P. 70239, 54506 Vandœuvre - lès - Nancy, France

Corresponding author: Marie-Christine Boiron, G2R, Nancy-Université, CNRS,
CREGU, Boulevard des Aiguillettes, B.P. 70239, 54506 Vandœuvre – lès - Nancy,
France

Phone: 33 3 83 68 47 30 fax: 33 3 83 68 47 01

Mail: marie-christine.boiron@g2r.uhp-nancy.fr

ABSTRACT

Fluid circulation at the basement / cover unconformities is of first importance for mass transfer and especially Pb-Zn, F, Ba, and U–deposits. This is typically the case for world-class Proterozoic U deposits (Athabasca, Canada, Kombolgie, Australia, Franceville, Gabon) basins, which show many similarities with younger Pb-Zn-F-Ba systems, where fluid mixing near the basement/cover unconformity is one of the key factors for the ore formation. Data have been compiled in order to compare a series of parameters (time gap between basin formation and metal deposit, origin and nature of the ore fluid, temperature of fluid end members in the case of mixing, style of migration). Pb-Zn Irish Paleozoic deposits, F-Pb-Zn-Ba deposits related to extensional tectonics from Spain, western France and Silesia and fluid movements related to a continental rifting on the example of the Rhine graben, have been considered.

Results show great similarities in all fluid systems: i) a wide range of fluid salinity indicating the lack of homogeneity of fluid chemistry at the scale of the reservoirs, ii) the deep penetration of brines through faults and dense networks of microfractures within the basement below the unconformity, iii) local fluid-rock interaction yielding to porosity increase and significant fluid chemistry changes, iv) a pulsatory fluid regime during fluid trapping, v) anisothermal fluid mixing revealed by a systematic temperature gap between the brines and the recharge fluids, vi) major stages of fluid movements facilitated by discontinuity opening in relation with later tectonic / telogenetic stages linked to major geodynamic events without relationships with sedimentation and burial, at the exception of a few cases characterized by the synchronous production, penetration of surface brines and ore genesis. The conditions of burial, penetration of brines in the Archean basement, suggest the need of thermal convection for the brine movements which could be linked to extensional tectonics.

Key words : fluid movement, brines, metal, unconformity, extensional tectonic

INTRODUCTION

Fluid circulation at the sedimentary cover basement unconformity is of first importance for mass transfer and especially Pb-Zn, F, Ba, Ag and U – ore deposits. In most cases, either the present day depth of the unconformity occurs at a few hundred metres or a few kilometres at maximum and indicating the loss of significant part of the sedimentary formations, or it is no more present. Such a loss of information on the overlying basin complicates largely the interpretation of the fluid and mass transfer processes including the most critical stages of ore formation. This is typically the case of the major U world – class deposits hosted by the Proterozoic basins. Such deposits occur close to the unconformity (U/C) between a Proterozoic sandstone cover and an Archean to Lower Proterozoic metamorphic basement. Main host basins are located in Saskatchewan (Athabasca Basin, Canada), Northern Territories, Australia (McArthur Basin, Alligator River Uranium Field), Oklo (Gabon). In all cases, only a minor part of the basin is preserved, as more than 5 to 7 kilometres above the unconformity are now eroded.

Although the nature of the ore process has been investigated since more than 30 years several aspects of the ore genesis remain not fully understood (references in Kyser & Cuney, 2008). Genetic models invoke large-scale circulation of basinal fluids and U uptake either from monazite-zircon paleoplacers in mid-Proterozoic sandstones, or from the basement, this yielding to two contrasted models: i) direct penetration of basinal fluids into the basement with U reduction at the contact with reducing lithologies and /or reducing fluids (Hoeve & Sibbald, 1978), ii) penetration of brines into the basement, U uptake in the basement itself and U deposition favoured by fluid mixing at the vicinity of major faults (Richard *et al.* 2010) There are several uncertainties on the genetic model of deposition, in particular on the relative timing and relationships between U deposition and geodynamic processes, the extension of the fluid movements, the relative role of water rock interaction versus fluid mixing for the uranium deposition.

1
2
3
4 1 The nature of the fluids, in particular high salinity Na-Ca brines with variable
5
6 2 Na/Ca ratios (Derome *et al.* 2003, 2005, 2007, Richard *et al.* 2010), the evidence of
7
8 3 brine mixing, the penetration of the sedimentary brines in the basement, the
9
10 4 localisation of the fluid migration near the unconformity display however, similarities
11
12 5 with fluid movements such as those reported in MVT like deposits (Leach *et al.*
13
14 6 2005) or more generally carbonate hosted Pb-Zn ores and F-Ba deposits at the
15
16 7 vicinity of the unconformity. Although such an analogy was not proposed in the past
17
18 8 for such deposits, the similarities between rather old, Mid-Proterozoic U deposits and
19
20 9 more recent fluid-rock systems in particular Mesozoic Pb-Zn-F-Ba deposits from
21
22 10 western Europe have encouraged us to develop a comparative study between the
23
24 11 two families of deposits.
25
26 12

27
28 13 The understanding of the Pb-Zn-F-Ba deposits was largely improved by the
29
30 14 direct study of paleofluid chemistry, and the consideration of the time relationships
31
32 15 between burial, diagenesis, fluid circulation related to metal deposition and the
33
34 16 geodynamic context. These data, generally dispersed in the literature, or gathered
35
36 17 together only for specific types of deposits, have been thus compiled and compared
37
38 18 on the example of major examples from western Europe: Pb-Zn Irish Paleozoic
39
40 19 deposits, F-Pb-Zn-Ba deposits related to extensional tectonics, associated with the
41
42 20 Atlantic ocean and Gascogne rifting, in Spain, western France and Silesia). In
43
44 21 addition, an intracontinental rift, the Rhine graben where Trias formations and the
45
46 22 basement were affected from Oligocene to present day times by large-scale fluid
47
48 23 flow, was also considered (Table 1). Besides, major accounts to the understanding of
49
50 24 fluid mixing were also considered from the literature in this comparative work. The
51
52 25 geodynamic context and style of fluid movement, although largely submitted to
53
54 26 discussions in the past 15 years, are much better known than in Proterozoic systems
55
56 27 and appears better constrained. The main goal of this paper is thus an attempt to
57
58 28 compare Proterozoic basins, hosting giant U-deposits, (the Alligator River Uranium
59
60 29 Field in Australia, the Athabasca basin in Canada and the Oklo deposit in Gabon)
30
31 30 with the reference Pb-Zn-F-Ba ore deposits for which the geodynamic context, and
style of fluid movement are better known than in Proterozoic systems. The objective

1
2
3 1 was to get key information and models on ore fluid movements in the upper
4 lithosphere and to evaluate their applicability to U deposits.
5
6
7 3

8
9 4 **GIANT U DEPOSITS RELATED TO THE UNCONFORMITY BETWEEN**
10 5 **PROTEROZOIC BASINS AND THEIR ARCHEAN BASEMENT**

11
12 6 The discovery in the 1980-1990's of several giant U deposits near the
13 unconformity between Proterozoic basins and their basement, in particular in the
14 Athabasca Basin, Saskatchewan, (Canada) and in Alligator River Uranium Field
15 (ARUF), McArthur Basin, Northern Territories, (Australia), has encouraged a rather
16 systematic evaluation of the nature of the ore fluids and of their origin. Such deposits
17 occur close to the unconformity between a Mid-Proterozoic sandstone cover and an
18 Archean to Lower Proterozoic metamorphic basement (see references in the
19 synthesis by Kyser & Cuney, 2008). Genetic models invoke large-scale circulation of
20 basinal Na-Ca rich fluids (Pagel, 1975; Pagel & Jaffrezic, 1977; Pagel *et al.* 1980;
21 Derome *et al.* 2003, 2005, 2007, Richard *et al.* 2010).
22
23
24
25
26
27
28
29
30
31
32
33

34 16 There are several uncertainties on the general model of deposition, in
35 particular on the timing of U deposition. Between the 1.7-1.8 Ga, the ages for the
36 sedimentation and the Grenville orogen, a few geodynamic events have occurred but
37 without clear effects on the basin which is located away from the major deformations.
38 Since the 80's for instance, ages of the U-ores for Proterozoic basins, have been
39 successively made older from 1.1 Ga up to 1.6 Ga due to the improvement of
40 analytical techniques which made possible the analysis of smaller and smaller
41 amount of ore considered as devoid of Pb loss due to coffinite alteration or uraninite
42 recrystallisation (Alexandre *et al.* 2009). Thus, in Canada, depending on the age of
43 the U-deposit, the Grenville, Berthoud (Sims & Stein, 2003), or Mazatzal (Amato *et*
44 *al.* 2008) orogens have been successively considered as the cause of fluid
45 movements or more recently as the cause of recrystallization of primary ores
46 (Alexandre *et al.* 2009). Difficulties to relate precisely a fluid event to a geodynamic
47
48
49
50
51
52
53
54
55
56
57
58
59
60

1 event characterized by a specific fluid signature and migration style complicate the
2 proposition of a metallogenic model.

3 4 **Alligator River Uranium Field (Australia)**

5 The Kombolgie sub-basin (northern Territory, Australia) overlies a basement
6 consisting of Archean and Early Proterozoic granito-gneisses (Nanambu Complex),
7 the Kakadu Group gneisses and quartzites, and the metasediments of the
8 epicontinental Cahill Formation. All these rocks underwent the Barramundi and the
9 Top End orogenies between 1870 and 1800 Ma (Page & Williams, 1988). A thick (up
10 to 1800 m presently preserved) unmetamorphosed detrital sequence composed of
11 fluvial and aeolian sandstones (the "Kombolgie Sub-Group") unconformably overlies
12 the crystalline and metamorphic basement and is dated 1822 and 1720 Ma (Sweet
13 *et al.* 1999). The youngest members of the Kombolgie Sub-group were deposited in
14 marine conditions, as suggested by the occurrence of glauconite and halite crystal
15 casts (Kyser *et al.* 2000), and by stromatolitic and evaporitic dolostone-sandstone
16 occurring in the McKay formation (Rawlings 1999). All uranium deposits are located
17 in basement rocks and ages are comprised between 1600 and 1650 Ma for the
18 Jabiluka, Nabarlek and Koongarra deposits (Maas 1989; Sm-Nd, Rb-Sr data on
19 uraninites, references in Kyser & Cuney, 2008).

20 The Kombolgie basin and its basement are characterized by hydraulic
21 breccias developed frequently along faults. Breccias consist of angular blocks of
22 sandstones cemented by nice euhedral drusy quartz crystals of rather exceptional
23 size up to 10 cm at their base. Two brines and a low salinity fluid showing clear
24 evidence of mixing with the brines (Derome *et al.* 2003) are observed in the drusy
25 quartz crystals from sealed faults (Table 2). The two brines consist of: i) a Na-rich
26 fluid with T_m ice ranging from -15 to -35 °C (mode around -25 °C) yielding to chlorinity
27 close to 5 moles/kg H₂O and a T_h between 90 and 160 °C (mode: 135 °C). Na/Ca
28 ratios determined by Laser Induced Breakdown Spectroscopy (LIBS) are around 8;
29 ii) a Ca-rich fluid characterized by T_m ice ranging from -35 to -52 °C (mode at -42 °C
30 and chlorinity between 5.6 and 6 moles/kg H₂O) and T_h between 100 to 140 °C
31 (mode 110 °C). Na/Ca ratios are closed to 0.1. The low to moderate salinity fluid
32 display T_m ice in the range of -0.3 to - 10 °C (mode at -2.5 °C) and T_h between 115
33 and 155 °C with a mode at 140 °C. Na/Ca ratio are variable in the range of 1 to 10.

The Athabasca uranium deposits

The Athabasca basin lies on Archean to Paleoproterozoic basement which consists of gneisses, metapelites and mafic to felsic intrusions affected by the Thelon –Talston (1.9 to 1.8 Ga) and Trans–Hudson (1.9 to 2.0 Ga) orogenies. The sedimentary sequence is now around 1500 meters at maximum but is thought to have reach 5 km based on pressure-temperature estimation from fluid inclusion studies (Pagel 1975, Derome *et al.* 2005). The sandstones as well as the basement display local quartz dissolution and precipitation and a major Mg-silicate alteration assemblage (Mg-rich di-octahedral chlorite (sudoite), Mg tourmaline (dravite) and Mg-illite). Ages proposed for the mineralization has been estimated in the range of 1510 to 1540 Ma (Cummings & Krstic, 1992, Alexandre *et al.* 2009). In quartz and carbonate veins, two to three phase inclusions are observed and consist in two brines: a sodium rich brine (T_m ice from -15 to -30 °C) and a calcium rich brine (T_m ice from -30 to -55 °C) which have circulated and mixed at the base of the basin and within the basement at the time of the formation of the uranium mineralisations at temperature close to 150 ± 30 °C (Table 2). The calcium rich brines were formed by interaction of the sodium-rich fluid interacting with the basement rocks. Both brines were originated from evaporated seawater as shown by the low Cl/Br ratios from Mc Arthur River, the Cl concentrations and other recent isotopic data including ³⁷Cl (Derome *et al.* 2005, Richard *et al.* 2009) (Fig. 1).

Olko natural reaction zones (Gabon)

The Francevillian sedimentary series unconformably overly the Archean crystalline basement represented by the north Gabon massif in the north and the Chaillu massif in the west (Gauthier-Lafaye, 1986, Gauthier-Lafaye & Weber, 1989). U/Pb, Rb/Sr and K/Ar age determinations of the granitoids (K-rich plutonites and diorites) from the Chaillu massif yield ages ranging from 2.88 to 2.4 Ga (Bonhomme *et al.* 1982). The Francevillian series is a 1 to 4 km thick, unmetamorphosed sequence of clastic and volcanoclastic sediments. The lithostratigraphic succession from the bottom to the top consists of: i) conglomerates and fine to coarse sandstones deposited in a fluvial to deltaic environment, ii) fine-grained marine sediments, mainly pelites and black shales, iii) massive dolomite and cherts

1
2
3 1 interbedded with black shales, iv) ignimbrites and epiclastic sandstones with
4 interbedded shales (Fig. 2).
5
6

7 3 Numerous quartz veins, often associated with wall-rock alteration, attest to
8 significant fluid movements along fractures during diagenesis of the Franceville
9 basin. Diagenesis of these formations resulted in a silicification of detrital quartz
10 grains and formation of authigenic illite and chlorite in the matrix (Gauthier-Lafaye,
11 1986, Gauthier-Lafaye & Weber, 1989). Fluids were related to the formation of
12 diagenetic minerals, generation of U ore deposits and the migration of hydrocarbons.
13 The extensional fractures in the Archean basement and the sandstones are filled by
14 a quartz- chlorite – calcite – sulphide and a U mineral assemblage (Mathieu *et al.*
15 2000). Mineralisations are dated around 1960 to 2050 Ma (Holliger, 1988).
16
17

18 12 Fluid circulating during the quartz - chlorite - calcite - sulphide and U mineral
19 stage can be divided in three major types with the following characteristics (Mathieu
20 *et al.*, 2000): i) high salinity Ca-Na rich brines displaying large Tm ice variations but
21 showing two groups from -63 to -46°C (Ca dominated fluid and Na/Ca ratio around
22 0.5) and from -36 to -27°C (Na dominated fluid and Na/Ca from 2 to 9) (Table 2). Th
23 ranges from 95 to 155°C. The highest salinity fluid displays the lowest Th; ii)
24 moderate salinity fluids with Tm ice in the range of -24 to -14°C and Th in between 90
25 to 160°C. These fluids are Na dominated fluids with Na/ Ca ratio from 2 to 5.5. iii) low
26 salinity fluids having Tm ice in the range of -1.3 to -5.5°C and Th between 100 to
27 175°C. Na is the major cation found in these fluids using LIBS, Ca being detected in
28 some inclusions yielding to Na/Ca around 25.
29
30
31
32

33 34 35 36 37 38 39 40 41 42 43 44 45 **BRINE MIGRATION IN RELATION WITH OCEANIC RIFTING**

46 47 **The Poitou High and Pb-F-Ba occurrences of the North-Western Massif** 48 49 **Central**

50
51 27 Significant fracture and porosity sealing characterizes the sedimentary cover-
52 basement interface in the north-western margin of the Aquitaine basin (France) close
53 to the north-western part of the French Massif Central. The Poitou High area is
54 located at the north-western border of the French Massif Central, corresponding to
55 the northern edge of the Aquitaine Basin. Below a ca. 150 m thick sedimentary cover
56 consisting of marine Lias and Dogger formations, the basement lithology is
57
58
59
60

1
2
3
4 1 dominated by plutonic rocks from the “Tonalitic Lineament” of the Limousin (Peiffer
5 1986; Shaw *et al.* 1993) containing multiple intrusions of medium-K calc-alkaline
6 2 tonalites and granodiorites dated around $350-360 \pm 5$ Ma (U-Pb on zircons; Bertrand
7 3 *et al.* 2001). Dolomite, calcite, fluorite, barite and quartz constitute most of the
8 4 fracture fillings attesting fluid circulation either in the sediments or in the basement
9 5 (Fourcade *et al.* 2002, Boiron *et al.* 2002, Cathelineau *et al.* 2004). These processes
10 6 (Fig. 3) are large scale as shown by the similarities of mineral sequences, fluid types
11 7 and general features of most of the F-Ba-Pb-Zn deposits located at the basement-
12 8 sedimentary cover interface all along the margins of the French Massif Central,
13 9 (Munoz *et al.* 1995, 1999, Ziserman 1980) as well as U reworking at Le Bernardan,
14 10 (Patrier *et al.* 1997).
15 11

16 12 Microthermometry and Raman microprobe investigations show the existence
17 13 of a single dominant fluid type ($\text{H}_2\text{O}-\text{NaCl}-\text{KCl}-\text{CaCl}_2 \pm \text{MgCl}_2$) in all primary two-
18 14 phase fluid inclusions from all the minerals of the infilling sequence. They show a
19 15 range of final ice melting temperatures from -3.8°C to -30.2°C (ice \pm hydrohalite
20 16 melting) (Table 2). The highest measured chlorinity is around 5.2 moles/kg. The
21 17 fluids are Na-dominated with a Ca contribution as indicated by the Na/ Ca ratio
22 18 around 4 ± 1 measured by LIBS. Homogenization temperatures are between 65°C
23 19 and 130°C for quartz and slightly lower for dolomite ($90-115^\circ$), barite ($85-115^\circ\text{C}$),
24 20 fluorite ($85-100^\circ\text{C}$) and calcite ($65-100^\circ\text{C}$) (Boiron *et al.* 2002).
25 21

22 **Albigeois fluorite deposits**

23 24 The most important fluorite district in France is considered to have formed
24 25 during Mesozoic times (150 Ma, Bonhomme *et al.* 1987) in relation with a third stage
25 26 of extensional tectonics occurring much after the main rifting period of the Atlantic
26 27 ocean, and before the Gascogne gulf rifting considered as coeval of the Aptian-
27 28 Albian ages. Munoz *et al.* (1999) put forward a model of continental brine circulation
28 29 (salinity: 20-26 wt % eq. NaCl, Ca-(Mg)-Na brines and Th between 85 and 170°C)
29 30 (Table 2), deeply in the basement and the formation of ores along faults where the
30 fluorite deposited as a consequence of temperature drop. Although the main ores

1 precipitate from waters having a $\delta^{18}\text{O}$ of around 0 to 3.2 ‰ and D/H in the range of –
2 15 to –63 ‰, authors considered that isotopic features are derived from meteoric
3 waters having underwent an isotopic shift by interaction with host rocks. This is the
4 main argument in favour of the continental origin of the brines. It can be also noted
5 that recent paleogeographic reconstruction and fission track data tend to indicate that
6 the French Massif Central was in great part covered by the sea during Lias and
7 Dogger times.

8 9 **The Malines Pb deposit**

10 The Malines Pb deposit in Cevennes (South-eastern part of the french Massif
11 Central) is an interesting example of a rather complex history, subject of several
12 controversies because hosted in old series (Cambrian in age) but affected by a
13 series of thermal - diagenetic - hydrothermal events that were difficult to date. Most
14 dates are relative and do not concern strictly the ores. Ambiguous textural
15 relationships attributed either as primary early diagenetic textures (karsts infilling
16 below the unconformity) or to epigenetic replacement, clay ages (Clauer & Chaudhuri,
17 1995) are interpreted as synchronous of the main fluid stage and considered as
18 general diagenetic stages without direct relationships with the ore deposition (Leach
19 *et al.* 2001). The remagnetization ages (60-50 Ma) are presented as related to
20 chemical process in direct link with the ore stage (Rouvier *et al.* 2001) but as
21 indicated by Muchez *et al.* (2005) no definitive argument of a direct genetic link with
22 the deposit of great mass of the Pb ores is given. The best relative chronological
23 indicators are based on geology (crosscutting relationships between ores and
24 sedimentary formation) and tectonics and put forward a post-Triassic age at
25 minimum, the most probable being an early Jurassic age (Macquar & Lagny, 1981,
26 Macquar *et al.* 1990, probably post-Hettangian, (Lotharingian to Bathonian) following
27 Charef & Sheppard, 1988) for the main ore stage and probably Kimmeridgian as
28 sulphide rich layers (sedex) are observed locally (Ming An *et al.* 1995). This does not
29 preclude an earlier pre-concentration stage. The main ore stage is characterized by
30 the mixing of a metal-rich brine (150 °C), considered as a connate water related to the
31 dewatering of the basin by Charef & Sheppard (1988), but which could be also linked
32 to fluid-rock interaction within the anhydrite-gypsum Triassic series overlying the
33 mineralized Cambrian formations, and a cooler dilute fluid (Table 3). As in many
34 other occurrences from the southern Massif Central, the thickness of the sedimentary

1
2
3 1 overburden cannot explain entirely the reached temperatures, and Charef &
4 Sheppard (1988) conclude to the existence of localized thermal anomalies, in part
5 2
6 3
7 4
8 5
9 6
10 7
11 8
12 9
13 10
14 11
15 12
16 13
17 14
18 15
19 16
20 17
21 18
22 19
23 20
24 21
25 22
26 23
27 24
28 25
29 26
30 27
31 28
32 29
33 30
34 31
35 32
36 33
37 34
38 35
39 36
40 37
41 38
42 39
43 40
44 41
45 42
46 43
47 44
48 45
49 46
50 47
51 48
52 49
53 50
54 51
55 52
56 53
57 54
58 55
59 56
60 57

6 **Mesozoic Fluorite veins (Spain)**

7 Fluorite veins developed in the Catalan costal range in faults affecting a
8 basement dominated by a series of calkcaline granodiorite - monzogranite
9 overlained by Triassic sediments including Keuper evaporites. Piqué *et al.* (2008)
10 conclude to the deep circulation of brines issued from the leaching of Mesozoic halite
11 and gypsum series by seawater and/or meteoric waters, within the basement where
12 brines uptook metals and gained K, Ca, Sr and Ba. Resulting Na-Ca-Cl (K-Mg) brines
13 are thought to have circulated during a late Jurassic-Early Cretaceous rifting stage
14 (dated 137 Ma) related to extensional tectonic and to the opening of the Atlantic
15 ocean (Piqué *et al.* 2008). The authors mention that this period is characterized by
16 elevated crustal temperatures during Mesozoic which can explain localized
17 convection (Juez-Larré & Andriessen, 2006). Although rich in metals, ore fluids
18 deposited fluorite, probably in relation with fluid mixing owing the large range of
19 salinities, but were not able to deposit metals due to the S content of the fluids
20 following Piqué *et al.* (2008).

21 The fluorite deposits in Asturias (Northern Spain) are hosted by Permo-
22 Triassic and Paleozoic rocks. Mineralisations occur in breccias and fractures and
23 consist of fluorite, barite, calcite, dolomite and quartz and small amounts of
24 sulphides. Mineralisations result of fluid mixing between deep brines with surficial
25 waters. Fluid movements and fluorite deposition occurred between late Triassic and
26 late Jurassic times (Sm-Nd age on fluorite at 185 ± 28 Ma, Sanchez *et al.* 2010) in
27 relation with rifting events associated with the Atlantic Ocean opening. Downward
28 penetration of brines into the basement, infiltration of surficial fluids and upwards
29 brine migration into the Mesozoic basin margins are the major processes to explain
30 the fluorite deposition in areas of fluid mixing (Sanchez *et al.* 2009).

The Pb-Zn deposit in Spain (Catalan coastal range and Basque Cantabrian area)

In the Maestrat basin, Zn-Pb deposits occurred in dolomitized Aptian limestones in the margins of the half-graben shape Penyagolosa sub-basin. Metal deposit is thought to be the result of the mixing between low temperature – low salinity (although it reaches up to 15 wt % eq NaCl) resident fluids enriched in sulphur may be migrated from below and issued from thermochemical sulphate reduction, and a high salinity brine of around 80-130°C supposed to be an evaporated seawater issued from the sabkha-like environments from Late Cretaceous/Early Paleocene, as suggested by the age of 62 ± 0.7 Ma for the mineralization process (Grandia *et al.* 2000, 2003a). The small thickness of the series at that time would imply large thermal discrepancies between the entering of fluids and the series, and probably larger convecting cells than those suggested by the authors in their sketch drawings, may be more than 4 km from the surface to reach temperatures of 130°C. In that case, the penetration and ascending migration of brines would be synchronous of the rifting stage (Fig. 4).

In sediment hosted Zn-Pb deposits of the Basque Cantabrian basin in Northern Spain, fluid mixing have been demonstrated based on microthermometric data and Na-K-Li-Cl-Br systematics on fluid inclusions (Grandia *et al.* 2003b). Fluids of different origins were involved in the mineralizing process: i) brines (25 wt % eq. NaCl) issued from seawater evaporation, ii) brines dissolving halite closed to salt domes, iii) low salinity fluids (seawater or fresh water) considered as diluted fluids.

The carbonate hosted Zn-Pb in Upper Silesia

Zn-Pb mineralizations occur on both sides of a Permian graben in Devonian to Jurassic rocks, especially in an early diagenetic/epigenetic dolosparite. More than 90% of the ores are hosted by the dolomitized series from Muschelkalk, but the age of the process is considered to be at less older than the upper Triassic, and from the lower Cretaceous as suggested by the age of 135 ± 4 Ma obtained on sphalerite. Ores form from highly saline Na-Ca brines (20-23 wt. % eq. NaCl, Table 2). Brines are thought to be evaporated seawater from Permian-Trias age which penetrated deeply in the Carboniferous units from the basement where they uptook metals and resulted through albitisation in Ca enriched brines. The expulsion from the basement would be much later during their extensional stages contemporaneous of the opening

1
2
3 1 of the Northern Atlantic ocean (Fig. 5). Following Heijlen *et al.* (2003), brines (70-
4 160°C) are not considered to have migrated through a gravity driven flow model as
5 2 originally suggested by Leach *et al.* (1996) but expelled along deep seated faults
6 3 affecting both basement rocks and their overlying sedimentary basins, in relation with
7 4 extension through a dilatational pump mechanism following the seismic model of
8 5 Muir Wood & King (1993).
9 6

10 7 11 8 **THE IRISH Pb-Zn DEPOSITS**

12 9 Irish deposits, which include Navan the largest Zn resource in Europe, are
13 10 considered to have been formed by the penetration of evaporated seawater, the
14 11 acquisition of metals by water rock interaction deeply in the continental crust down to
15 12 5 to 10 km (Russel 1978), and the mixing of this ascending brine with surficial brines
16 13 rich in H₂S issued from bacterial activity within the lower carboniferous limestones
17 14 overlying the lower paleozoic basement, in fractured zones (Blakeman *et al.* 2002,
18 15 Wilkinson *et al.* 2005). This model emphasizes the role of rift zones and local
19 16 extensional tectonics and considers the topographic flow models proposed by
20 17 Hitzmann & Beaty (1996) as unsuitable for the Irish deposits. It puts forward also the
21 18 role of thermo-haline density driven convection as the main engine for the fluid
22 19 movement (Fig. 6). The age (350 Ma, in Wilkinson *et al.* 2005) of these deposits is
23 20 in favour of a model of brine circulation nearly coeval with their formation as
24 21 Mississippian evaporites which are present in the sedimentary sequence, a feature at
25 22 variance of most other deposits presented in our comparative study. The
26 23 relationships between the process of seawater evaporation and the heating
27 24 mechanism of the surface brine is however not fully elucidated in terms of
28 25 paleogeography, the extension of the Mississippian sea controlling the area and
29 26 volume of evaporated seawater formed at that time and able to penetrate from the
30 27 surface, and depth-temperature relationships controlling the possible temperatures
31 28 reached near the marine sediment – seawater interface.
32 29

33 30 **INTRACONTINENTAL RIFTING: THE SOULTZ-SOUS-FORÊTS GEOTHERMAL** 34 31 **AREA, RHINE GRABEN (EASTERN FRANCE)**

35 32 The Soultz-sous-Forêts geothermal plant is located in the Rhine Graben which
36 33 constitutes part of the continental rift extending from Frankfurt (Germany) to Basel
37 34 (Switzerland). It formed during the Oligocene by large-scale extension related to

1
2
3 1 mantle upwelling (Rousset *et al.* 1993). The north-western part of the Rhine Graben
4 is filled by an asymmetric sedimentary cover ranging from Triassic to Oligocene
5
6 2 is filled by an asymmetric sedimentary cover ranging from Triassic to Oligocene
7 overlying an Hercynian fractured granitic basement. The sedimentary cover is
8
9 3 overlying an Hercynian fractured granitic basement. The sedimentary cover is
10 composed of thick Tertiary series, mainly represented by marls and clays. It overlies
11
12 4 composed of thick Tertiary series, mainly represented by marls and clays. It overlies
13 Triassic sediments which are subdivided into the three classical lithofacies: Keuper,
14
15 5 Triassic sediments which are subdivided into the three classical lithofacies: Keuper,
16 Muschelkalk and about 300 m of Buntsandstein sandstones (Fig. 7). The main
17
18 6 Muschelkalk and about 300 m of Buntsandstein sandstones (Fig. 7). The main
19 granite body is an Hercynian monzogranite dated at 331 ± 9 Ma (U-Pb method,
20
21 7 granite body is an Hercynian monzogranite dated at 331 ± 9 Ma (U-Pb method,
22 Alexandrov *et al.* 2001) with no equivalent at the surface.
23
24 8 Alexandrov *et al.* 2001) with no equivalent at the surface.

25
26 9 At Soultz-sous-Forêts, past to recent fluid movements are recorded by series
27
28 10 of healed or sealed micro- to macrostructures, which provide evidence of a rather
29 continuous self-sealing of the open space (Dubois *et al.* 1996, Smith *et al.* 1998,
30
31 11 of healed or sealed micro- to macrostructures, which provide evidence of a rather
32 Cathelineau & Boiron, 2009). This circulation is believed to be at the origin of drastic
33
34 12 Cathelineau & Boiron, 2009). This circulation is believed to be at the origin of drastic
35 changes in heat transfer in this area, explaining that the present day temperature
36
37 13 changes in heat transfer in this area, explaining that the present day temperature
38 gradient decreases from $0.09-0.10$ °C.m⁻¹ in the sedimentary cover to unexpected
39
40 14 gradient decreases from $0.09-0.10$ °C.m⁻¹ in the sedimentary cover to unexpected
41 values of $0.04-0.01$ °C.m⁻¹ in the upper part of the fractured granites (Clauser &
42
43 15 values of $0.04-0.01$ °C.m⁻¹ in the upper part of the fractured granites (Clauser &
44 Villinger, 1990, Person & Garven, 1992). In drill holes, the sedimentary cover and the
45
46 16 Villinger, 1990, Person & Garven, 1992). In drill holes, the sedimentary cover and the
47 granite display altered zones characterized by dense network of veins, and alteration
48
49 17 granite display altered zones characterized by dense network of veins, and alteration
50 of the host rocks (Ledésert *et al.* 1999, Sausse, 2002, Sausse *et al.* 2006). Veins
51
52 18 of the host rocks (Ledésert *et al.* 1999, Sausse, 2002, Sausse *et al.* 2006). Veins
53 are filled by quartz or barite and healed microfissures reveal a successive self-
54
55 19 are filled by quartz or barite and healed microfissures reveal a successive self-
56 sealing of the rocks.
57
58 20 sealing of the rocks.

59
60 21 Previous studies of paleofluid circulation in EPS-1 (Exploration Puits Soultz)
61
62 22 drill hole have shown the circulation of moderate to highly saline fluids either in the
63 sedimentary cover and in the basement down to 2200 m depth (Dubois *et al.* 1996,
64
65 23 sedimentary cover and in the basement down to 2200 m depth (Dubois *et al.* 1996,
66 2000) and in the GPK2 (Géothermie Puits Kutzenhausen) deep drilling in the
67
68 24 2000) and in the GPK2 (Géothermie Puits Kutzenhausen) deep drilling in the
69 basement up to 5057 m (Cathelineau & Boiron, 2009). In the two studied zones
70
71 25 basement up to 5057 m (Cathelineau & Boiron, 2009). In the two studied zones
72 either in sandstones and granite closed to the unconformity or in the deep granite
73
74 26 either in sandstones and granite closed to the unconformity or in the deep granite
75 samples, fluids show a large range of T_m ice: -31.6 to -0.2 °C in the shallowest levels
76
77 27 samples, fluids show a large range of T_m ice: -31.6 to -0.2 °C in the shallowest levels
78 and from -24.6 °C to -0.1 in the deep granite. These data indicate a probable fluid
79
80 28 and from -24.6 °C to -0.1 in the deep granite. These data indicate a probable fluid
81 mixing between two end-members: a brine enriched in divalent cations and a rather
82
83 29 mixing between two end-members: a brine enriched in divalent cations and a rather
84 dilute fluid. All inclusions homogenized to the liquid phase between 100 °C and
85
86 30 dilute fluid. All inclusions homogenized to the liquid phase between 100 °C and
87 184 °C. The measured T_h range between 100 °C and 165 °C for the shallow studied
88
89 31 184 °C. The measured T_h range between 100 °C and 165 °C for the shallow studied
90 zone and from 150 °C and 185 °C at 5057m. The T_m ice - T_h diagrams (Fig. 8) show
91
92 32 zone and from 150 °C and 185 °C at 5057m. The T_m ice - T_h diagrams (Fig. 8) show
93 that the fluid inclusions with the highest salinity (i.e. the lowest T_m ice) have the
94
95 33 that the fluid inclusions with the highest salinity (i.e. the lowest T_m ice) have the
96 lowest homogenization temperatures, and the low salinities correspond to the highest
97
98 34 lowest homogenization temperatures, and the low salinities correspond to the highest

1
2
3 1 Th. The mixing trend found at 5057 m is sub-parallel to the mixing trend found for
4
5 2 samples from a depth ranging from 1430 m to 2207 m. The two extreme salinities are
6
7 3 similar in both cases, but a difference in Th of approximately 35-40°C is found
8
9 4 between the two sets of samples.

10 5 Although not precisely dated, a series of F-Ba showings are observed on both
11
12 6 sides of the Rhine graben (Vosges and Schwarzwald) in the basement and the
13
14 7 margins of Mesozoic basins. A part of them have been considered on the basis of
15
16 8 structural relationships as Tertiary to recent and linked to the graben activity (Lüders
17
18 9 1994, Franzke & Lüders, 1993), or linked to earlier rifting stages during Mesozoic. In
19
20 10 Schwarzwald district, fluorite-barite-quartz vein formation are related to the
21
22 11 circulation of seawater derived fluids having strongly interacted with the basement
23
24 12 where they gained chlorine and calcium (21-26 wt % eq. NaCl) and mixed along
25
26 13 faults with surface-derived meteoric dilute fluids at temperature in the range of 100-
27
28 14 180°C (Lüders & Franzke, 1993, Baatartsogt *et al.* 2007).
29
30 15

31 16 **PALEOFLUID COMPOSITIONS AND ORIGIN**

32
33 17 A great part of the data was already published in each case study (references
34
35 18 below) but these data are homogenized to illustrate the main differences or
36
37 19 similarities between main fluid types, in order to compare to literature data on
38
39 20 reference deposits. Microthermometric data, cation and halogen ratios are
40
41 21 compared and presented in figures 8 to 12 and table 2.
42
43 22

44 23 **Chlorinity and Tm ice ranges**

45
46 24 A remarkable feature of a part of the study cases, eg the Oklo and Northern
47
48 25 territories U deposits, the F-Ba deposits from Massif central, and the Rhine graben
49
50 26 examples is the nearly continuous trend of chlorinity between two end-members (Fig.
51
52 27 8 and 9): a dilute end-member with the highest Tm ice values close to 0°C, and a
53
54 28 brine end-member. Fluid inclusions with variable Tm ice within a same quartz
55
56 29 overgrowth, or set of fluid inclusion planes (FIP), were found and considered as
57
58 30 nearly coeval, or corresponding to the same fluid event. This indicates that at each
59
60 31 increment of sealing or trapping within a same vein, fluids trapped reflect the
32
33 32 compositional inhomogeneity of the migrating fluids. Such variations are particularly
well shown by the Soultz veinlets and deep granite sample FIP, formed within a

1 relatively short period after Oligocene under nearly constant temperature conditions
2 but characterized by inclusions with almost all chlorinities from brines to dilute fluids.
3 In the western Massif Central and at Soultz, the lowest T_m ice values are around –
4 32°C , as fluids are NaCl dominated brines. The high chlorinity brine with low Na/Ca
5 ratios were mostly found in Proterozoic basins. In the later, two contrasted cases
6 were observed: i) the Athabasca basin where brines with similar chlorinity and large
7 variation in Na/Ca ratio resulting in a large T_m ice range (-6 to -30°C) do not show
8 dilution evidences and ii) the Northern Territories U deposits (Australia) and Oklo
9 where mixing of two brines is also accompanied by a dilution.

11 **Na/Ca-Na/K ratios**

12 One of the most striking features of the inclusion fluids from the studied U-Pb-
13 Zn- F-Ba deposits is their low Na/K and Na/Ca ratios. Brines with low Na/Ca ratio
14 were also reported in more recent systems such as waters from the KTB (Möller *et*
15 *al.* 2005) but with much lower chlorinities (Fig. 10).

16 Both ratios reach values near 1 in most of evolved brines, and a large part of
17 the paleofluids have Na/K ratio below 20 with mean values lower than 10 and Na/Ca
18 ranging from 1 to 10. The low Na/K ratio are much lower than those predicted by Na-
19 K geothermometers or found in hydrothermal systems for a temperature range of 90
20 -150°C , e.g. values ranging from 50 to 150 (Verma & Santoyo, 1997).

23 **Halogen ratios**

24 In most studied cases, a part of the Cl/Br ratios are mostly lower than that of
25 seawater and may correspond to brines having passed the halite saturation, and in
26 some instances the epsomite saturation (Fig. 11). It can be noted that data points
27 were calculated for mean values as the bulk leachates mix all fluid inclusions, but
28 that the chlorinity range is larger in individual samples. Low Cl/Br ratios are typical of
29 primary brines, e.g. brines issued from seawater evaporation. In Mid-Proterozoic
30 basins such as those from Northern Territories, Mc Arthur (Canada), Cl/Br values are
31 low whatever the chlorinity, in the range of 100 to 400, and not scattered. In other
32 Athabasca deposits, a rather wide range of values from 200 up to 800 have been
33 measured (Richard, 2009). At Soultz or in the NW Massif Central, Cl/Br ratio are
34 more scattered, indicating either a mixing of primary brines having a large range of

1
2
3 1 Cl/Br ratios, a rather improbable hypothesis or a mixing of primary brines with
4 secondary brines as data points are significantly above the mixing lines between
5 2 seawater (or dilute fluids such as meteoric recharge fluids) and an evaporite brine
6 3 having passed the epsomite saturation. The existence of secondary brines with
7 4 higher Cl/Br ratio is easily conceivable as dilute fluids or seawater entering the fluid
8 5 system may have interacted with the evaporite formations as described elsewhere
9 6 (Hanor & Mcintosh, 2007). Ranges and values of Cl/Br ratios found in ore fluid
10 7 inclusions in all studied sites is in favour of an evaporitic source for chlorine and of
11 8 partial to significant mixing of primary and secondary brines. In a few cases,
12 9 secondary brines predominate (Fig. 12) (Spanish Pb-Zn-F deposits Catalan and
13 10 Cantabrian coastal range, Grandia *et al.* 2003 a and b, Piqué *et al.* 2008, Sanchez *et*
14 11 *al.* 2009).
15 12
16 13

14 **Homogenisation temperatures and distribution of Tm-Th pairs**

15 Figures 8 and 9 are a comparison of Tm-Th pairs for a series of studied cases.
16 The common feature to all FI populations is the Tm-Th trend between two end-
17 16 members: a brine with a Th around 100°C and a dilute fluid end-member with a
18 17 higher Th, around 30 to 40°C higher than the Th of the brine.

19 A scattering of Th for a given Tm ice is observed for some FI populations, this
20 19 being attributed to several reasons: i) unavoidable effects of stretching, ii) the
21 20 presence in U deposits of radiolytic gases such as H₂ which cause generally an
22 21 increase in Th, a rather common observation in most U deposits, iii) superimposition
23 22 of non-synchronous fluid populations at different temperatures, iv) fluctuation in fluid
24 23 pressure above the hydrostatic pressure, a process which can be mostly considered
25 24 in a deep seated fluid system when the unconformity reaches a depth of 4-5 km.

26 It can be noted that fluid pressure may be estimated from the consideration of the
27 26 depth of the unconformity at the time of the deposition, assuming the nature of the
28 27 pressure (hydrostatic or lithostatic). The depth is generally inferred from temperature
29 28 estimates, considering geothermal gradients and assuming the nature of the fluid
30 29 pressure. For depths lower than 5 km, the pressure is likely to be hydrostatic, but at
31 30 lower depths, intermediate or fluctuating pressures could be recorded. This
32 31 uncertainty of the nature of the fluid pressure makes more difficult the interpretation
33 32 of Th values. In the case of all trends characterized by a large and continuous range
34 33 of Tm ice correlated with Th (Soultz, Oklo), it is highly probable that pressures can be

1 interpreted as hydrostatic. Alternatively, rather large scattering in Th for a given fluid
2 salinity can be interpreted as the result of alternating changes in fluid pressure above
3 the hydrostatic pressure assuming that the temperature was constant. This is the
4 case of Athabasca U deposits.

6 DISCUSSION

7 The evolution of the fluid system responsible for the formation of carbonate
8 hosted deposits in the sedimentary basins, and metal deposition in the basement
9 near the unconformity is summarized in the figure 13 and table 3. Main stages are
10 discussed below.

12 Brine origin

13 High chlorinities reaching 4 to 6 moles/kg, Cl/Br ratios much lower than the
14 seawater ratio (Cl/Br < 600 molar ratio), indicate a probable primary origin of the
15 brines, e.g., brine issued from the evaporation of seawater. In the case of ores found
16 within an outcropping basement, or in the case of sedimentary basin only known by a
17 thin remaining sequence at the top of the basement, evaporitic brines are mostly
18 suspected on a geochemical basis. Almost no evidence of evaporite or localized
19 relics of such formations is found at present, this being due either to the dissolution of
20 salt since the basin formation, or to the erosion and complete loss of these
21 formations. Secondary brines are also suspected in a number of cases explaining the
22 difficulty to find the pristine evaporite formations. In the case of old systems, such as
23 mid-Proterozoic basins, a great part of the basins is now eroded (more than 3
24 kilometers following P-T reconstructions, see Derome et al. 2003, 2005), and
25 evaporite formations only found sporadically, frequently at great distances of the
26 mineralized areas. In Australian Mid-Proterozoic basins, a few occurrences are
27 described away from the studied zones such as the evaporitic dolostones in the
28 MacKay formation in the south-eastern part of the McArthur basin (northern
29 territories, Rawlings 1999). In addition, evaporites are very sensitive to leaching,
30 resulting in secondary brines, and these evaporites may not be visible anymore.

31 In most other cases considered in this paper, evaporites were found or
32 supposed close to the basement (Fig 1 to 7): Hettangian series at the unconformity
33 in the NW Massif Central (Poitou High), Trias evaporites near the unconformity in the
34 Rhine graben, Silesia, most Spanish examples. In the Poitou High, evidences of

1
2
3 1 evaporites are found at a certain distance or for relics of evaporite layers such as
4
5 2 boxworks of gypsum in the case of the Infra-Liassic series, the Hettangian evaporite
6
7 3 layers being found at more than 100 km to the south in the Angouleme region, and
8
9 4 Trias evaporite even at higher distances. In the Rhine graben, although salt layers
10
11 5 are easily identified within the Trias series from Alsace, drill holes did not crosscut
12
13 6 salt formations at Soultz. In other occurrences cited, at the exception of the Irish
14
15 7 deposits, evaporites from Trias are lying above the basement and can be considered
16
17 8 as a key factor of the process. These observations are in favour of a rather wide
18
19 9 brine migration away from their “mother” formation.
20

21 11 **Why deep penetration of brines within the basement is so important?**

22
23 12 **Brines – basement rocks interactions:** The penetration of basinal fluids
24
25 13 within the basement has been previously discussed (Yardley et al, 2000, Cathles &
26
27 14 Adams 2005), and described in southern Norway (Munz *et al.* 1995, Gleeson *et al.*
28
29 15 2003), in Spain (Piqué *et al.* 2008), and in various places in Europe (Bouch *et al.*
30
31 16 2006, and see review in Muchez et al. 2005). The depth reached by the brines
32
33 17 remains in a great number of cases rather hypothetical as the style of migration.
34
35 18 Recent detailed studies of granitoids from Athabasca, and deep samples from the
36
37 19 Soultz granite provide some keys for the understanding of the process of brine
38
39 20 migration. The deep penetration of brines within the basement through faults is thus
40
41 21 associated with an intimate fluid invading through the matrix permeability. Dense
42
43 22 networks of opened and interconnected microfractures are revealed by the healed
44
45 23 brine inclusion plane networks within the basement (granites or granitoïds).
46
47 24 Microfracturing such as at Soultz is observed in the whole granite down to 5 km
48
49 25 depth (Cathelineau & Boiron 2009), and allow brines to interact deeply with the host
50
51 26 rocks. FIP from deep samples are dominated by recent reservoir fluids and fluid
52
53 27 salinities depict the full range of mixing between the sedimentary brine and the hot
54
55 28 dilute fluids. Thus, either sets of micro-fissures were formed and healed at depth
56
57 29 since the Oligocene or the inherited FIP from earlier stages were reopened and
58
59 30 healed by the main reservoir fluids.
60

31
32
33
34 Such a microfracturing is also found in basement rocks from Saskatchewan
(Athabasca basin, Mercadier 2008, Mercadier *et al.* 2009). There, the early
microfractures, from the late Hudsonian retrograde metamorphism were reopened
and healed by evaporitic brines, indicating a fully pervasive brine infiltration through

1 rocks. The efficiency of the process needs the formation, or re-opening of
2 microfissures at the time of the brine movements, the healing of the cracks which
3 ensured the trapping of the paleobrine indicating that fissures formed probably
4 during repeated microsismic events. This penetration of the brine in the
5 microfractured pathways is one of the key factors for metal extraction. The studies of
6 brines within the basement rock microfractures are however scarce and would merit
7 further development to generalize such a process.

8 **Metal extraction:** The presence of an eroded basement with regolith or
9 weathered surface generally found down to a few tens of meters below the
10 unconformity is the second key factor of the metal extraction: after peneplanation,
11 within the weathered part of the outcropping basement, supergene alteration affects
12 most feldspars and phyllosilicates and their deep alteration is a major cause of
13 element release. Pb and Ba are released from feldspars, F and probably Zn from
14 biotite, U from uraninite in biotite and monazite, and subsequent sorbed onto clays
15 and Fe-Ti oxides and hydroxides. In Western Europe, the main metal reservoir is
16 thus the weathered Hercynian terranes, "peneplaned" at Trias and affected by
17 supergene alteration. The latter produced a thick weathered and oxidized zone, well
18 exposed in basement quarries showing the unconformity (Mauzé-Toarçais for
19 instance, for the Poitou High). Metal can be easily extracted by brines later on, once
20 most of the metal bearers are deeply altered. It can be noted that In the case of Ag
21 and Ni-Co-As deposits from Morocco, the metals are extracted from weathered
22 ultramafic rocks (middle Precambrian) and transported later on by brines during late
23 Trias or early Lias (Essarraj *et al.* 1998, 2005) near the unconformity following the
24 same process. Brines penetrating the weathered basement have all the features
25 (temperature, chloride content) required for an optimal metal solubilisation and
26 complexation, as shown by the increased metal concentrations in fluids at increasing
27 chlorinity and temperature (Yardley, 2005). The high metal concentrations (Cu, Pb,
28 Zn, Fe, Mn, ...) of sedimentary brines was reported in most carbonate hosted base
29 metal deposits (Heijlen *et al.* 2008, Piqué *et al.* 2008, Wilkinson *et al.* 2009).

30 In the case of uranium, Hecht & Cuney (2000) have documented the
31 dissolution of accessory minerals (zircons and monazite) in the presence of brines
32 which constitute an additional source of U at the time of brine circulation. LA-ICPMS
33 analyses have shown that brines from the Athabasca basin could transport significant
34 amounts of U which range from 10 to some hundred of ppm (Richard *et al.* 2010).

1
2
3 1 When interacting with the basement, chemical features of the sodium
4 2 dominated brine may drastically evolve towards Ca-K-(Mg) rich brines. High Ca/Na
5 3 ratios are generally interpreted as the result of a Ca/ Na exchange through mineral-
6 4 fluid interaction such as albitisation, or Na-metasomatism at greater depth (review in
7 5 Kharaka & Hanor, 2004). The complete conversion of a Na dominated evaporitic
8 6 brine into a Ca dominated brine is however still difficult to interpret. Such Ca rich
9 7 fluids were found either in the present day waters sampled in the basements (KTB for
10 8 instance, Möller *et al.* 2005), or in the Saskatchewan deposits where they are
11 9 considered as the main brine responsible for U extraction and deposition.
12 10

11 Fluid mixing

12 **Mixing of two or more fluids in the major fluid pathways:** Two major fluid
13 13 types are generally found in cemented pathways: i) one or more brines frequently
14 14 identified as primary brines issued from evaporated seawater having passed halite
15 15 saturation and expelled during compaction stages or tectonic stages linked to major
16 16 geodynamic events. ii) dilute fluids corresponding to recharge meteoric (or marine)
17 17 fluids or local resident fluids issued from multiple evolution. In all studied cases,
18 18 brines display a large range of composition, and in most cases a large range of
19 19 chlorinity indicative of mixing between brines and dilute fluid end-members. The
20 20 variety of salinity-temperature pairs indicates that at each stage of fluid circulation
21 21 and healing of the micro-fissures, a distinct rate of mixing between the two fluids is
22 22 registered. These different rates of mixing show also that the reservoir fluids were not
23 23 fully homogenized at the time of healing of the micro-fissures. The dilute end-
24 24 member of the mixing trends is likely considered as a recharge fluid of meteoric
25 25 origin. Pristine features of surface fluids are however generally lost, as the $\delta^{18}\text{O}$ of
26 26 the fluid estimated from the $\delta^{18}\text{O}$ values of quartz are in general typical of fluids
27 27 buffered by sediment mineral assemblages. $\delta^{18}\text{O}$ values are in most cases, ranging
28 28 from 0 to 4 ‰ (Table 2). Exceptions concern fluid flow in large drainage faults, such
29 29 as those described by Smith *et al.* (1998) at Soultz. Very similar Th-Tm ice trends
30 30 with nearly complete series of chlorinities between the two end-members were found
31 31 in a part of the studied basins as already presented in the preceding paragraph and
32 32 indicate that the mixing process occurred in most of the studied locations. In some of
33 33 the listed examples, e.g. the Asturias F district (Sanchez *et al.* 2009), the Maestrat

1 basin, (Grandia et al. 2003a), authors do not report clear trend of mixing between a
2 dilute end member and a brine but series of trapping of fluids covering a large range
3 of chlorinities. It can be noted that in other unconformity deposits such as those from
4 Saskatchewan (Athabasca basin), the dilute fluid end-member is almost lacking and
5 fluid mixing concerns only the two brines end-members, the Na-dominated and the
6 Ca-dominated (Derome et al. 2005, Richard *et al.* 2010). The lack of chemical
7 homogenization of the circulating fluids seems however to characterize most of the
8 basins considered in our comparative study.

9
10 ***Cold fluids and hot ascending fluids in thermal disequilibrium with host***
11 ***formations?*** In a part of the study cases, a systematic temperature gap is recorded
12 between the two fluid end-members, generally a few tens of degree cooler than the
13 recharge fluids. The presence of slightly colder brines indicates that downward
14 penetration of sedimentary brines tends to cool the deep reservoir fluids. The 35-
15 40°C gap between the estimated temperature for brines that record the hotter dilute
16 fluids, may correspond to more than one kilometer difference in depth, assuming a
17 mean thermal gradient of about 30°C /km, if the two fluids are in thermal equilibrium
18 with the host rocks in their respective reservoirs. The temperature difference between
19 the brine and the hotter dilute fluid in a given zone, e.g. the area of fracture sealing is
20 indicative of an anisothermal mixing. At Soultz, the anisothermal mixing is found in all
21 parts of the granite reservoir, as shown by the variety of salinity-temperature pairs
22 and the T_m-T_h trend which are typical of each depth interval (Cathelineau & Boiron,
23 2009).

24 In a part of the Proterozoic basins (northern territories, Australia, Athabasca
25 basin, Canada and Oklo, Gabon), the range of homogenization temperatures is
26 rather similar to those recorded at Soultz in the upper parts of the reservoir (2 km) or
27 in the north Massif Central. Temperatures can therefore be either converted into
28 depths of 4-5 km assuming regular thermal gradients, or can be considered as
29 temperatures representative of abnormal thermal gradients at much shallower depths
30 of 1-3 km such as those recorded in the Rhine graben.

31 Significant exceptions are: i) data obtained on Maestrat basin where brines at
32 130°C (23 wt% eq. NaCl) mixed with a cooler and more dilute fluid (Grandia *et al.*
33 2003a), ii) Asturias where no definite mixing trends were obtained (Sanchez et al.,

1
2
3 1 2009), and Malines where the dilute fluid is cooler (70°C) than the brines (150°C)
4 (Charef & Sheppard, 1988).
5
6
7
8

9
10 4 **Brine-host rock interactions in the deposit area (mineral dissolution,**
11 5 **silicification, dolomitization, and Mg alterations):** Two main cases may be
12 6 distinguished: i) alteration within sedimentary formation which are generally
13 7 dominated by dolomitization. In the sedimentary cover, in limestones especially,
14 8 dolomitization and calcite dissolution creating porosity were observed in a great
15 9 number of cases. The main driving force for this process is linked to the high Mg
16 10 concentration of the evaporated seawater which is the main cause of the calcite
17 11 dissolution and the replacement by dolomite. The resulting fluid is depleted in Mg and
18 12 enriched in Ca. ii) Mg-silicate alteration within the basement. It is worth noting that
19 13 Mg rich evaporite fluids are responsible for the intense Mg-metasomatism which
20 14 affects the basement. Mg alteration from U deposits is characterized either by the
21 15 crystallization of chlorites (Oklo, Northern territories, Australia), or by a sudoite-Mg
22 16 illite assemblage in Athabasca (Kister *et al.* 2006, Mercadier *et al.* 2009). These
23 17 alteration display similar mineral assemblage than the main talc deposits such as the
24 18 Trimouns deposit in Pyrenees which results from the circulation of evaporitic brine
25 19 during the Gascogne gulf extension (Boulvais *et al.* 2006, Boiron *et al.* 2007). As Ca-
26 20 Mg brines are generally enriched also in potassium, K-alteration (adularisation) may
27 21 also occur at the top of the basement near the unconformity in the Poitou high.
28
29
30
31
32
33
34

35
36
37
38
39
40
41 22 Large silicification characterizes the main ascending pathways and is
42 23 generally favoured by the cooling and mixing of hot fluids with lower temperature
43 24 dilute fluids. The main driving force at the origin of massive quartz precipitation is
44 25 thus the decrease of the quartz solubility at decreasing temperature (Crerar &
45 26 Anderson, 1971). Thus, little amount of quartz is precipitated in Canada unconformity
46 27 deposits, where no hot dilute recharge fluids were found, compared to Australian
47 28 deposits where large amounts of quartz formed by dilution and cooling of recharge
48 29 fluids in faults, above the unconformity U deposits. Rather significant silicification are
49 30 found at Soultz (quartz filled faults, Smith *et al.* 1998) and some deposits from the
50 31 Poitou High (quartz-galena infillings from Melle, La Charbonnière and Chatenet
51 32 quartz-fluorite veins, Boiron *et al.* 2002). Silicification is thus a major indicator of
52 33 temperature change, sometimes coupled with dilution in pathways favouring the
53 34 convection of external fluids.
54
55
56
57
58
59
60

1 Anisothermal mixing of brines with dilute fluids favours the precipitation of
2 different mineral assemblages depending on the availability of metals, and the
3 presence of not of sulphur. Dilution process provokes the destabilisation of metal
4 complexes, especially U and Pb chlorides. The availability of sulphur is however a
5 key parameter and two main sources may be invoked: the bioreduction of sulfates
6 (BSR) which is invoked for instance in Irish deposits for the S enrichment of one of
7 the two mixed brines, the colder and most superficial one responsible of the Zn
8 deposit (Wilkinson *et al.*, 2005), and the thermal reduction of sulphates (Machel
9 2001) which can produced H₂S and be therefore one of the factor controlling metal
10 deposition when some sedimentary formation reached the oil window (case of the
11 Maestrat basin, Grandia *et al.* 2003 a and b). In cases where one fluid involved in the
12 mixing was not sufficiently rich in sulfur, mixing caused mainly the precipitation of
13 fluorite and carbonate, the spent fluid remaining enriched in metals. Such fluids may
14 have kept their potential for a metal deposition in more favourable environments.
15 Metal deposits may be found, therefore, away from the fluorite deposits, as
16 suspected by Piqué *et al.* (2008) for the central Catalan coastal range deposits.

17 18 **Geodynamic context**

19 The cause of fluid migration remains frequently unknown due to difficulties in
20 dating precisely the ore events and to relate precisely the origin of the fluid migration
21 to specific geodynamic events. These relationships are almost impossible to prove to
22 have occurred on great distances once the basin or the belt is eroded. Extensional
23 versus compressional tectonic movements were thus largely discussed in the
24 literature to explain MVT deposits. The debate on gravity driven fluid movements
25 proposed by Leach *et al.* (2005) for a series of deposits is in part linked to the
26 weakness of the method used for dating the process. Thus, in the case of Cevennes
27 Pb deposits, after a few decades of models favouring a rather old karst infilling, the
28 deposits were alternately considered as linked to compressional tectonics related to
29 the Pyrenean orogeny (60 Ma) on the basis of remagnetization (Rouvier *et al.* 2001),
30 or linked to previous extensional stages during Malm (see discussion, In Muechez *et*
31 *al.* 2005). In most cases where rather young ages were proposed (135 Ma in Silesia,
32 185 Ma in Asturias, 60 Ma in Cevennes) it has been impossible to link precisely the
33 remagnetization of minerals to the ore formation. Models were therefore hardly
34 discussed : Heijlen *et al.* 2003, for Silesia, Wilkinson *et al.* 2005, for Irish deposits,

1
2
3 1 Muechez *et al.* 2005 for a variety of deposits hosted by Mesozoic formation over
4 Europe including Cevennes, put forward the many arguments in favour of reliable
5 ages (Sm-Nd on fluorite for instance) and robustness of models invoking the link
6 between extensional tectonics and ore formation rather than younger stages related
7 to orogeny (pyrenean, or alpine events for Mesozoic deposits).
8
9

10
11
12 6 The origin of hot fluids can be found in localized abnormal heat flows, and
13 convection cells favoured by faults crosscutting both the basement and the
14 sedimentary cover. In the Poitou region, up to now, such convection cells were
15 mostly inferred for the lower Lias formation, where metal deposits were considered
16 as syn-sedimentary. In that case, hydrothermalism was considered as synchronous
17 with the Atlantic ocean opening. New geochronological data tend to indicate that
18 these convection cells were active after the main stage of lower Lias sedimentation
19 e.g. around 140-155 Ma (Fourcade *et al.* 2010). The major stages of fluid movements
20 in relation with porosity increase due to localized mineral dissolution, or discontinuity
21 opening are thus not related with early diagenesis or main stages of compaction, but
22 correspond to later events linked to major geodynamic events. Most fluid events
23 described in this paper occur in between 50 and 200 Ma later after the
24 sedimentation.
25
26
27
28
29
30
31
32
33
34

35 36 37 20 **Style of migration: deep downward penetration and convective cells**

38
39 21 The main driving forces for the convection of brines are: i) the role of “relief “
40 area as already proposed for MVT deposits (Leach *et al.* 2001) and ii) abnormal heat
41 flow which characterizes rifting tectonics. The patterns of palaeofluid circulation are
42 shown in Figures 1 to 7: i) a major system of laterally migrating brines at the
43 basement - sedimentary cover interface where both sandstones and the upper part of
44 the basement had a high permeability, acquired for the basement by weathering
45 during the emersion period, ii) local convective cells rooted at least at more than 5
46 km depth, involving low salinity fluids (presumably surface derived, likely migrating,
47 through basement from structural highs) generally centered on horst fault systems, or
48 faults (reverse in the case of the unconformity U deposits), iii) deep downward
49 penetration of brines which accounts for the introduction of large amounts of chlorine
50 in the basement microfractures. In the western Massif Central, brines are considered
51 to have migrated along the unconformity below an impermeable cover formation, and
52 then mixed locally with recharge fluids in fault systems.
53
54
55
56
57
58
59
60

1
2
3 1 Numerical hydrological modelling of basins aquifers by Evans *et al.* (1991)
4 shows that: i) either the density differences related to salinity contrast between the
5 2 fluid reservoirs are the primary driving forces for fluid flow when sediments
6 3 surrounding salt contain a dilute fluid, or ii) thermal effects are necessary to get the
7 4 convection in brine dominated aquifers. The mixing of hot recharge dilute fluids and
8 5 colder brines indicates that dilute fluids are able to convect from remoted areas, and
9 6 can be channellized along faults. Meteoric waters are heated at depth and their
10 7 density allows them to ascend along drainage faults such as extensional faults (horst
11 8 and graben systems). Brines are flowing downward to great depth due to their
12 9 specific density.
13 10

14 11 In all studied cases, the hydraulic conductivity of the stratigraphic units
15 12 influences the brine regime on a regional scale, as shown by the specific role of the
16 13 conglomerate and sandstone above the regolith or weathered basement, which
17 14 constitute in all studied cases a major aquifer above the fractured basement, below
18 15 cap rocks such as clay rich formations (Toarcian marls in Poitou, clay-rich formations
19 16 in the Rhine graben, FB clay formation at Oklo). Such controls are already shown in
20 17 similar contexts in the North German basin (Magri *et al.* 2009).
21 18

22 19 **Lessons from rather recent systems for the understanding of very old** 23 20 **brine migrations**

24 21 *Analogies in fluid chemistry:* fluids found in giant U deposits have the same
25 22 features than brines evolved by basement interactions and found in most carbonate
26 23 hosted deposits or unconformity related F-Ba-Pb-Zn deposits from western Europe
27 24 and in basement rocks.

28 25 *Depth of brine penetration within the archean below the unconformity:* there
29 26 are no limits to the brine penetration within the fractured basement, as shown by
30 27 young systems such as those related to the continental rifting of the Rhine graben.
31 28 The analogy between the multiple microfissuring of archean rocks and healing by
32 29 sedimentary brines and the process observed at Soultz is remarkable. The infiltration
33 30 of brines below the unconformity in Athabasca may therefore have reached 5 km.

34 31 *Role of thermal convection:* The example of Soultz and Massif Central provide
35 32 some keys for the understanding of the old systems where little is known on the
36 33 dynamics of fluids and on the geometry of fluid pathways. In NW-Australia as well as
37 34 in the NW Massif Central, the dilution of brines in fault systems near the unconformity

1 is observed. In both cases, the origin of hot recharge waters may be found in analog
2 models such as the Soultz geothermal area where recharge fluids are driven from
3 rather remote lateral sources in outcropping areas (meteoric fluid recharge).

4 Similar fluid migration affects the Oklo area (Fig. 2): the main deposit is
5 located at the vicinity of a major fault of the Mounana basement horst, which was
6 considered as related to a double continental rift (Fanceville-Lastourville basin and
7 Okondia rift) on both sides of the Ondii-Dambi horst (Gauthier-Lafaye 1986). Main
8 stages of fluid migration are considered to be related to the main extensional phase
9 around 2.05 Ma (Gancarz 1978). The formation of hydraulic breccia attests of
10 contrasted fluid pressure (Gauthier-Lafaye 1986). The recharge fluids, as at Soultz,
11 likely infiltrated in the basement horst relief (Chaillu granite), and mixed with brines
12 and oil fluids from the sedimentary aquifers (FA conglomerates) along horst faults.

13 It is highly probable that the formation of giant U deposits in Saskatchewan
14 was not possible if not linked to a specific geodynamic event which could have
15 caused : i) the microfissuring and reactivation of preexisting micropermeability and
16 faults, ii) the localized heat flows which were necessary for brine convection, as no
17 fluid density contrast characterize the two main brines found in these deposits.

18 *Pulsatory fluid regime*: the wide variety of salinity during fluid trapping between
19 the brines which penetrate downward in the basement and the ascending fluids was
20 found at Oklo and in Northern Territories (Australia) but not in Saskatchewan. The
21 analogy with recharge fluids commonly found in relation with convective systems
22 driven by localized heat flows and recharge from emerged zone is only possible in
23 the two latter cases. The lack of homogeneity of the brine composition is in favour of
24 successive inputs of brine within the main fault system, and repeated pulses
25 following models well known in aquifer systems in relation with micro- or macro-
26 seismicity.

27 28 **ACKNOWLEDGEMENTS**

29 This paper has benefited from different works carried out at CREGU-G2R by
30 J. Mercadier, D. Derome and R. Mathieu and from fruitful discussions with M. Cuney,
31 D.A. Banks and S. Fourcade. The authors thank CNRS and Areva NC for financial
32 support (BDI PhD grant for A. Richard). Areva NC and Cameco are also
33 acknowledged for providing samples and scientific collaborations. S. Gleeson, P.

1
2
3 1 Mucchez and B. Yardley are warmly acknowledged for their constructive comments
4 and editorial handling.
5
6

7 REFERENCES

8
9 4 Alexandre P, Kyser K, Thomas D, Polito P, Marlat J (2009) Geochronology of
10 unconformity-related uranium deposits in the Athabasca basin, Saskatchewan,
11 Canada and their integration in the evolution of the basin. *Mineralium Deposita*,
12 **44**, 41-59.
13
14

15
16 8 Alexandrov P, Royer JJ, Deloule E (2001) 331 ± 9 Ma emplacement age at the
17 Soultz monzogranite (Rhine Graben basement) by U/Pb ion-probe zircon dating
18 of samples from 5km depth. *Comptes Rendus de l'Académie des Sciences*
19 *Paris*, **332**, 747-754.
20
21

22
23 12 Amato JM, Bouillon AO, Serna AM, Sanders AE, Farmer GL, Gehrels G.E., Wooden
24 JL (2008) Evolution of the Mazatzal province and the timing of Mazatzal
25 orogeny: Insights from U-Pb geochronology and geochemistry of igneous and
26 metasedimentary rocks in southern New Mexico. *GSA Bulletin*, **120**, 328-346.
27
28

29
30 16 Baatartsogt B, Schwinn G, Wagner T, Taubald H, Beitter T, Markl G (2007)
31 Contrasting paleofluid systems in the continental basement ; a fluid inclusion
32 and stable isotope study of hydrothermal vein mineralization, Schwarzwald
33 district, Germany. *Geofluids*, **7**, 123-147.
34
35

36
37 20 Bertrand JM, Leterrier J, Cuney M, Brouand M, Stussi JM, Delaperrière E, Virlogeux
38 D (2001) Géochronologie U-Pb sur zircon de granitoides du Confolentais, du
39 massif de Charroux-Civray (seuil du Poitou) et de Vendée. *Géologie de la*
40 *France*, **1-2**, 167-189.
41
42

43
44 24 Blakeman RJ, Ashton JH, Boyce AJ, Fallick AE, Russell MJ (2002) Timing of
45 interplay between hydrothermal and surface fluids in the Navan Zn + Pb
46 orebody, Ireland : Evidence from metals distribution trends, mineral textures
47 and $\delta^{34}\text{S}$ analyses. *Economic Geology*, **97**, 73-91.
48
49

50
51 28 Boiron MC, Cathelineau M, Banks DA., Buschaert S, Fourcade S, Coulibaly Y, Boyce
52 A, Michelot JL (2002) Fluid transfers at a basement/cover interface. Part II:
53 Large-scale introduction of chlorine into the basement by Mesozoic basinal
54 brines. *Chemical Geology*, **192**, 121-140.
55
56

57
58 32 Boiron MC, Cathelineau M, Dubessy J, Fabre C, Boulvais P, Banks DA (2007) Na-
59 Ca-Mg rich brines and talc formation in the giant talc deposit of Trimouns
60

- 1
2
3 1 (Pyrenees): Fluid inclusion chemistry and stable isotope study. *Proceeding of*
4 *the ECROFI XIX meeting*, Bern, Juillet 2007.
5 2
6
7 3 Bonhomme M, Gauthier-Lafaye F, Weber F (1982) An example of Lower Proterozoic
8 sediments. *Precambrian Research*, **18**, 87-102.
9 4
10 5 Bonhomme M, Baubron JC, Jebrak M (1987) Minéralogie, géochimie, terres rares et
11 âge K-Ar des argiles associées aux minéralisations filoniennes. *Chemical*
12 *Geology*, **65**, 321-339.
13 7
14
15 8 Bouch JE, Naden J, Shepherd TJ, McKervey JA, Young B, Benham AJ, Sloane HJ
16 (2006) Direct evidence of fluid mixing in the formation of stratabound Pb-Zn-Ba-
17 F mineralisation in the Alston Block, North Pennine Orefield (England).
18 *Mineralium Deposita*, **41**, 821-835.
19 10
20
21 11 Boulvais P, De Parseval P, D'Hulst A, Paris P (2006) Carbonate alteration associated
22 with talc-chlorite mineralization in the eastern Pyrenees, with emphasis on the
23 St Barthelemy massif. *Mineralogy and Petrology*, **88**, 499-526.
24 13
25
26 14 Carpenter AB, Trout ML, Pickett EE (1974) Preliminary report on the origin and
27 chemical evolution of lead- and zinc-rich oil field brines in central Mississippi.
28 *Economic Geology*, **69**, 1191-1206.
29 17
30
31 18 Cathelineau M, Boiron MC, (2009) Downward penetration and mixing of sedimentary
32 brines and dilute hot waters at 5 km depth in the granite basement at Soultz-
33 sous-Forêts (Rhine graben, France). *CR. Geosciences*, in press.
34 19
35
36 20 Cathelineau M, Fourcade S, Clauer N, Buschaert S, Rousset D, Boiron MC, Meunier
37 A, Lavastre V, Javoy M (2004) Multistage paleofluid percolations in granites: A
38 stable isotope and K-Ar study of fracture illite from Vienne plutonites (N.W. of
39 the french Massif Central). *Geochimica Cosmochimica Acta*, **68**, 2529-2542.
40 22
41
42 23 Cathles LM, Adams JJ (2005) Fluid flow and petroleum and mineral resources in the
43 upper (<20km) continental crust. *Economic Geology*, 100th Anniversary volume,
44 77-110.
45 27
46
47 28 Charef A, Sheppard SMF (1988) The Malines Cambrian carbonate-shale-hosted Pb-
48 Zn deposit, France: Thermometric and isotopic (H, O) evidence for pulsating
49 hydrothermal mineralization. *Mineralium Deposita*, **23**, 86-95.
50 30
51
52 31 Clauer N, Chaudhuri S (1995) Inter-basinal comparison of the diagenetic evolution of
53 illite/ smectite minerals in buried shales on the basis of K-Ar systematics. *Clays*
54 *and Clay Minerals*, **44**, 818-824.
55 32
56
57 33
58
59
60

- 1
2
3 1 Clauser C, Villinger H (1990) Analysis of conductive and convective heat transfer in a
4 sedimentary basin, demonstration for the Rhine Graben. *Geophysical Journal*
5 *International*, **100**, 393-414.
6
7 2
8 3
9 4 Crerar DA, Anderson GM (1971) Solubility and solvation reactions of quartz in dilute
10 hydrothermal solutions. *Chemical Geology*, **8**, 107–122.
11 5
12 6 Cumming GL, Krstic D (1992) The age of unconformity-related uranium
13 mineralization in the Athabasca Basin, northern Saskatchewan. *Canadian*
14 *Journal of Earth Sciences*, **29**, 1623-1639.
15 7
16 8
17 9 Derome D, Cuney M, Cathelineau M, Fabre C, Dubessy J, Bruneton P, Hubert A
18 (2003) A detailed fluid inclusion study in silicified breccias from the Kombolgie
19 sandstones (Northern Territory, Australia): inferences for the genesis of middle-
20 Proterozoic unconformity-type uranium deposits. *Journal of Geochemical*
21 *Exploration*, **80**, 259-275.
22 12
23 13
24 14 Derome D, Cathelineau M, Cuney M, Fabre C, Lhomme T, Banks DA (2005) Mixing
25 of sodic and calcic brines and uranium deposition at the McArthur River,
26 Saskatchewan, Canada. A Raman and Laser-Induced Breakdown
27 Spectroscopic study of fluid inclusions. *Economic Geology*, **100**, 1529-1545.
28 15
29 16
30 17 Derome D, Cathelineau M, Fabre C, Boiron MC, Banks DA, Lhomme T, Cuney M
31 (2007) Paleo-fluid composition determined from individual fluid inclusions by
32 Raman and LIBS: Application to mid-Proterozoic evaporitic Na-Ca brines
33 (Alligator Rivers Uranium Field, northern territories Australia). *Chemical*
34 *Geology*, **237**, 240-254
35 18
36 19
37 20
38 21
39 22
40 23 Dubois M, Ayt Ougougdal M, Meere P, Royer JJ, Boiron MC, Cathelineau M (1996)
41 Temperature of paleo- to modern self-sealing within a continental rift basin : the
42 fluid inclusion data (Soultz – sous – Forêts, Rhine graben, France). *European*
43 *Journal of Mineralogy*, **8**, 1065-1080.
44 24
45 25
46 26
47 27
48 28
49 29
50 30
51 31
52 32
53 33
54 34
55 35
56 36
57 37
58 38
59 39
60 40

- 1
2
3 1 Essarraj S, Boiron MC, Cathelineau M, Banks DA, El Boukhari A, Chouaidi MY
4 (1998) Brines related to Ag deposition in the Zgounder silver deposit (Anti-Atlas,
5 2 Morocco). *European Journal of Mineralogy*, **10**, 1201-1214.
6 3
7 4 Essarraj S, Boiron MC, Cathelineau M, Banks DA, Benaharref M (2005) Penetration
8 5 of surface – evaporated brines into the Proterozoic basement and deposition of
9 6 Co and Ag at Bou Azzer (Morocco): Evidence from fluid inclusions. *Journal of
10 7 African Earth Sciences*, **41**, 25-39.
11 8
12 9 Evans DG, Nunn JA, Hanor JS (1991) Mechanisms driving groundwater flow near
13 10 salt domes. *Geophysical Research Letters*, **18**, 927-930.
14 11
15 12 Fisher RS, Kreitler CW (1987) Geochemistry and hydrodynamics of deep-basin
16 13 brines, Palo Duro Basin, Texas, USA. *Applied Geochemistry*, **2**, 459-476.
17 14
18 15 Fontes JC, Matray JM (1993) Geochemistry and origin of formation brines from Paris
19 16 Basin, France. 1. Brines associated with triassic salts. *Chemical Geology*, **109**,
20 17 149-175.
21 18
22 19 Fourcade S, Boiron MC, Cathelineau M, Ruffet G, Clauer N, Belcourt O, Deloule E,
23 20 Coulibaly Y, Banks DA, (2010) A major Late-Jurassic/Lower Cretaceous
24 21 episode of fluid motion in the basement of western France: Precise Ar-Ar
25 22 dating, fluid chemistry, and geodynamic context. *Lithos*, submitted.
26 23
27 24 Fourcade S, Michelot JL, Buschaert S, Cathelineau M, Freiburger R, Coulibaly Y,
28 25 Aranyossy JF (2002) Fluids transfer at the basement/cover interface. Part I:
29 26 Subsurface recycling of basement trace carbonate (Vienne granitoids, France).
30 27 *Chemical Geology*, **192**, 99-119.
31 28
32 29 Franzke HJ, Lüders V (1993) Formation of hydrothermal fluorite deposits in the
33 30 southern Black Forest (SW Germany). Part I : Structural control. . In *Current
34 31 Research in Geology Applied Deposits*, Fenoll Hach Ali, Torres Ruiz & Gervilla
35 32 Ed., Granada, 719-722.
36 33
37 34 Gancarz J (1978) U-Pb age (2.05 10⁹ years) of the Oklo uranium deposit. Natural
38 35 Fission reactors. *IAEA Symposium Proceedings*, 513-520.
39 36
40 37 Gauthier-Lafaye F (1986) Les gisements d'uranium du Gabon et les réacteurs
41 38 d'Oklo. Modèle métallogénique de gîtes à fortes teneurs du Protérozoïque
42 39 inférieur. *Mémoire Sciences Géologiques*, **78**, 206 p.
43 40
44 41 Gauthier-Lafaye F, Weber F (1989) The Francevillian (Lower Proterozoic) uranium
45 42 ore deposit of Gabon. *Economic Geology*, **84**, 2267-2268.
46 43
47 44
48 45
49 46
50 47
51 48
52 49
53 50
54 51
55 52
56 53
57 54
58 55
59 56
60 57

- 1
2
3 1 Gleeson SA, Yardley BWD, Munz IA, Boyce AJ (2003) Infiltration of basinal fluids into
4 high-grade basement, South Norway: sources and behaviour of waters and
5 brines. *Geofluids*, **3**, 33-48.
6
7
8 4 Grandia F, Asnerom Y, Getty S, Cardellach E, Canals A (2000) U-Pb dating of MVT
9 ore –stage calcir. Implications for fluid flow in a Mesozoic extensional basin from
10 Iberian peninsula. *Journal of Geochemical Exploration*, **69-70**, 377-380.
11
12 7 Grandia F, Cardellach E, Canals A, Banks DA (2003a) Geochemistry of fluids related
13 to epigenetic carbonated hosted Zn-Pb deposits in the Maestrat basin, Eastern
14 Spain: Fluid inclusion and isotope (Cl, C, O, S, Sr) evidence. *Economic
15 Geology*, **98**, 933-954.
16
17 11 Grandia F, Canals A, Cardellach E, Banks DA, Perona J (2003b) Origin of ore –
18 forming brines in sediments – hosted Zn-Pb deposits of the Basque –
19 Cantabrian basin, Northern Spain. *Economic Geology*, **98**, 1387-1411.
20
21 14 Hanor JS, McIntosh JC (2007) Diverse origins and timing of formation of basinal
22 brines in the Gulf of Mexico sedimentary basin. *Geofluids*, **7**, 227-237.
23
24 16 Hecht L, Cuney M (2000) Hydrothermal alteration of monazite in the Precambrian
25 crystalline basement of the Athabasca basin (Saskatchewan, Canada):
26 Implications for the formation of unconformity – related uranium deposits.
27 *Mineralium deposita*, **35**, 791-795.
28
29 20 Heijlen W, Muechez P, Banks DA, Schneider J, Kucha H, Keppens E (2003)
30 Carbonate-hosted Zn-Pb deposits in upper Silesia, Poland: Origin and evolution
31 of mineralizing fluids and constraints on genetic models. *Economic Geology*,
32 **98**, 911-932.
33
34 24 Heijlen W, Banks DA, Muechez P, Stensgard BM, Yardley BWD (2008) The nature of
35 mineralizing fluids of the Kipushi Zn-Cu deposit, Katanga, Democratic Republic
36 of Congo: Quantitative fluid inclusion analysis using Laser Ablation ICP-MS and
37 bulk crush-leach methods. *Economic Geology*, **103**, 1459-1482.
38
39 28 Hitzman MW, Beaty DW (1996) Geological setting of the Irish Zn –Pb (Ba-Ag)
40 orefield . in Sangster DF ed., *Society of Economic Geology Special Publication*,
41 **4**, 112-143.
42
43 31 Holliger P (1988) Ages U/Pb définis in-situ sur oxydes d'uranium à l'analyseur
44 ionique: méthodologie et conséquences géochimiques: *Comptes Rendus de
45 l'Académie des Sciences, Paris*, **307**, 367-373.
46
47
48
49
50
51
52
53
54
55
56
57
58
59
60

- 1
2
3 1 Hoeve J, Sibbald T (1978) On the genesis of rabbit Lake and other unconformity-type
4 uranium deposits in northern Saskatchewan, Canada. *Economic Geology*, **73**,
5 2 1450-1473.
6
7 3
8
9 4 Juez-Larré J, Andriessen PAM (2006) Tectonothermal evolution of the northeastern
10 margin of Iberia since the break up of Pangea to present, revealed by low-
11 5 temperature fission-track and (U-Th)/He thermochronology : a case history of
12 6 the catalan coastal ranges. *Earth and Planetary Science Letters*, **243**, 159-180.
13 7
14 8 Kharaka YK, Maest AS, Carothers WW, Law LM, Lamothe PJ, Fries TL (1987)
15 9 Geochemistry of metal-brines from Central Mississippi Salt Dome basin (USA).
16 10 *Applied Geochemistry*, **2**, 543-561.
17
18 11 Kharaka YK, Hanor JS (2004) Deep fluids in continents: I Sedimentary basins.
19 12 *Treatise on Geochemistry*, **5**, 499-540.
20
21 13 Kister P, Laverret E, Quirt D, Cuney M, Patrier Mas P, Beaufort D, Bruneton D (2006)
22 14 Mineralogy and geochemistry of the host-rocks alterations associated with the
23 15 Shea-Creek unconformity-type uranium deposits (Athabasca basin,
24 16 Saskatchewan, Canada). Part 2: Regional-scale distribution of the Athabasca
25 17 sandstone matrix minerals. *Clays and Clay Minerals*, **54**, 295-313.
26
27 18 Kyser TK, Renac C, Hiatt E, Holk G, Durocher K (2000) Comparison of diagenetic
28 19 fluids in Proterozoic Basins, Canada and Australia: implications for long
29 20 protracted fluid histories in stable intracratonic basins. GEOCANADA 2000,
30 21 Calgary.
31
32 22 Kyser TK, Cuney M (2008) Unconformity-related uranium deposits. In Recent and
33 23 not-so-recent developments in uranium deposits and implications for
34 24 exploration. Kyser and Cuney Eds., *Mineralogical Association of Canada*, **39**,
35 25 161-219.
36
37 26 Leach DL, Viets JG, Kozkowski A, Kibitlewski S (1996) Geology, geochemistry and
38 27 genesis of the Silesia – Cracow zinc-lead district, southern Poland. *Society of*
39 28 *Economic Geologists Special Publication*, **4**, 171-181.
40
41 29 Leach DL, Bradley D, Lewchuk MT, Symons DTA, de Marsily G, Brannon J (2001)
42 30 Mississippi Valley-type lead-zinc deposits through geological time: Implications
43 31 from recent age-dating research. *Mineralium Deposita*, **36**, 711-740
44
45 32 Leach DL, Sangster DF, Kelley K.D, Large RR, Garven G, Allen CR, Gutzmer J,
46 33 Walters S (2005) Sediment – hosted lead-zinc deposits : a global perspective.
47 34 *Economic Geology*, 100th Anniversary volume, 261-607.

- 1
2
3 1 Ledésert B, Berger G, Meunier A, Genter A, Bouchet A (1999) Diagenetic-type
4 reactions related to hydrothermal alteration in the Soultz-sous-Forêts granite.
5 *European Journal of Mineralogy*, **11**, 731-741.
6
7 3
8
9 4 Lüders V (1994) Geochemische Untersuchungen an Gangarterialen aus dem
10 Bergbaurevier Freiamt-Sexau und dem Badenweiler-Quarzriff, Schwarzwald. In
11 : *Die Erz-und Mineralgänge im alten Bergbaurevier "Freiamt-Sexau", Mittlerrer*
12 *Schwarzwald* (eds Storch DH, Werner W), *Abhandlungen des Geologischen*
13 *Landesamtes Baden – Württemberg*, **14**, 191-205.
14
15 8
16
17 9 Lüders V, Franzke HJ (1993) Formation of hydrothermal fluorite deposits in the
18 southern Black Forest (SW Germany). Part II: Geochemical features. In *Current*
19 *Research in Geology Applied Deposits*, Fenoll Hach Ali, Torres Ruiz & Gervilla
20 Ed., Granada, 739-742.
21
22 11
23
24 13 Ludwig KR, Grauch RI, Nutt CJ, Nash JT, Frishman D, Simmons KR (1987) Age of
25 uranium mineralization at the Jabiluka and Ranger deposits, Northern Territory,
26 Australia: new U-Pb Isotope evidence. *Economic Geology*, **82**, 857-874.
27
28 15
29
30 16 Maas R (1989) Nd-Sr isotope constrains on the age and origin of unconformity-type
31 uranium deposits in the Alligator Rivers Uranium Field, Northern Territory,
32 Australia. *Economic Geology*, **84**, 64-90.
33
34 18
35 19 Machel HG (2001) Bacterial and thermochemical sulfate reduction in diagenetic
36 settings: old and new insights. *Sedimentary Geology*, **140**, 143–175.
37
38 21 Macquar JC, Lagny P (1981) Minéralisations Pb-Zn "sous inconformité" des séries de
39 plate-formes carbonatées. Exemple du gisement de Trèves (Gard). Relations
40 entre dolomitisations, dissolutions et minéralisations. *Mineralium Deposita*, **16**,
41 293-307.
42
43 23
44
45 24 Macquar JC, Rouvier H, Thieberoz J (1990) Les minéralisations Zn, Pb, Fe, Ba, F
46 péri-cévenoles: cadre structuro – sédimentaire et distribution spatio –
47 temporelle. *Documents BRGM*, **183**, 143-158.
48
49 27
50
51 28 Magri F, Bayer U, Pekdegger A, Otto R, Thomsen C, Maiwald U (2009) Salty
52 groundwater flow in the shallow and deep aquifer systems of the Schleswig-
53 Holstein area (North German Basin). *Tectonophysics*, **470**, 183-194.
54
55 30
56
57 31 Mathieu R (1999) Reconstitution des paléocirculations fluides et des migrations
58 élémentaires dans l'environnement des réacteurs nucléaires naturels d'Oklo
59 (Gabon) et des argilites de Tournemire (France). Unpubl. Thesis, INPL, Nancy,
60 519 p.
34

- 1
2
3 1
4
5 2 Mathieu R, Cuney M, Cathelineau M (2000) Geochemistry of paleofluids circulation in
6
7 3 the Franceville basin and around Olko natural reaction zones (Gabon). *Journal*
8
9 4 *of Geochemical Exploration*, **69-70**, 245-249.
- 10 5 Mercadier J (2008) Conditions de genèse des gisements d'uranium associés aux
11
12 6 discordance protérozoïques et localises dans les socles. Exemple du socle du
13
14 7 bassin d'Athabasca (Saskatchewan, Canada). Unpub. Thesis, Nancy Université,
15
16 8 353 p.
- 17 9 Mercadier J, Richard A, Boiron MC, Cathelineau M, Cuney M (2009) Brine
18
19 10 penetration in the basement rocks of the Athabasca Basin through
20
21 11 microfracture networks at the P-Patch U deposit (Canada). *Lithos*, doi:
22
23 12 10.1015/j. lithos 2009.11.010.
- 24 13 Ming-An H, Disnar JR, Sureau JF (1995) Organic geochemical indicators of
25
26 14 biological sulphate reduction in the early diagenetic Zn-Pb mineralization: The
27
28 15 Bois-Madame deposit (Gard, France). *Applied Geochemistry*, **10**, 149-435.
- 29 16 Möller P, Woith H, Dulski P, Lüders V, Erzinger J, Kämpf H, Pekdeger A, Hansen B,
30
31 17 Lodemann M, Banks DA, (2005) Main and trace elements in the KTB-VB fluid:
32
33 18 composition and hints to its origin. *Geofluids*, **5**, 28-41.
- 34 19 Muech P, Heijlen W, Banks D, Blundell D, Boni M, Grandia F, (2005) Extensional
35
36 20 tectonics and the timing and formation of basin –hosted deposits in Europe. *Ore*
37
38 21 *Geology Reviews*, **27**, 241-267.
- 39 22 Muir Wood R, King GCP (1993) Hydrothermal signatures of earthquake strain.
40
41 23 *Journal of Geophysical Research*, **98**, 22 035-22 068.
- 42 24 Munoz M, Boyce AJ, Courjault-Rade P, Fallick AE, Tollon F (1995) Multi-stage fluid
43
44 25 incursion in the Palaeozoic basement-hosted Saint-Salvy ore deposit (NW
45
46 26 Montagne Noire, southern France), *International Journal of Rock Mechanics*
47
48 27 *and Mining Science & Geomechanics Abstracts*, **32**, 5, 202A.
- 49 28 Munoz M, Boyce AJ, Courjault-Rade P, Fallick AE, Tollon F (1999) Continental
50
51 29 basinal origin of ore fluids from southwestern Massif Central fluorite veins
52
53 30 (Albigeois, France): evidence from fluid inclusion and stable isotope analyses,
54
55 31 *Applied Geochemistry*, **14**, 447-458
- 56 32 Munz, I.A., Yardley, B.W.D., Banks, D.A., and Wayne, D. (1995) Deep penetration of
57
58 33 sedimentary fluids in basement rocks from southern Norway : Evidence from
59
60

- 1 hydrocarbon and brine inclusions in quartz rocks. *Geochimica Cosmochimica*
2 *Acta*, **59**, 239-254.
- 3 Page RW, Williams IS (1988) Age of the Barramundi Orogeny in northern Australia
4 by means of ion microprobe and conventional U-Pb zircon studies. *Precambrian*
5 *Research*, **40-41**, 21-36.
- 6 Pagel M (1975) Détermination des conditions physico-chimiques de la silicification
7 diagénétique des grès Athabasca (Canada) au moyen des inclusions fluides.
8 *Comptes Rendus de l'Académie des Sciences, Paris*, **280**, 2301-2304.
- 9 Pagel M, Jaffrezic H (1977). Analyses chimiques des saumures des inclusions du
10 quartz et de la dolomite du gisement d'uranium de Rabbit Lake (Canada).
11 Aspect méthodologique et importance génétique. *Comptes Rendus de*
12 *l'Académie des Sciences, Paris*, **284**, 113-116.
- 13 Pagel M, Poty B, Sheppard SMF (1980) Contribution to some Saskatchewan
14 uranium deposits mainly from fluid inclusion and isotopic data. *International*
15 *Uranium Symposium on the Pine Creek Geosyncline*, 639-654.
- 16 Patrier P, Beaufort D, Bril H, Bonhomme M, Fouillac AM, Aumaitre R., (1997)
17 Alteration-mineralization at the Bernardan U deposit (Western Marche, France);
18 the contribution of alteration petrology and crystal chemistry of secondary
19 phases to a new genetic model. *Economic Geology*, **92**, 448 - 467.
- 20 Pauwels H, Fouillac C, Fouillac AM (1993) Chemistry and isotopes of deep
21 geothermal saline fluids in the upper Rhine Graben: Origin of compounds and
22 water-rock interactions. *Geochimica Cosmochimica Acta*, **57**, 2737-2749.
- 23 Peiffer MT (1986) La signification de la ligne tonalitique du Limousin. Son implication
24 dans la structuration varisque du Massif Central français. *Comptes Rendus de*
25 *l'Académie des Sciences, Paris*, **303**, 305-310.
- 26 Person M, Garven G (1992) Hydrologic constraints on petroleum generation within
27 the continental rift basins; theory and application to the Rhine Graben.
28 *American Association of Petroleum Geology Bulletin*, **76**, 468-488.
- 29 Piqué A, Canals A, Grandia F, Banks DA, (2008) Mesozoic fluorite in NE Spain
30 record regional base metal-rich brine circulation through basin and basements
31 during extensional events. *Chemical Geology*, **257**, 139-152.
- 32 Polito PA, Kyser KK, Jackson MJ (2006) The role of sandstone diagenesis and
33 aquifer evolution in the formation of uranium and zinc –lead deposits, southern

- 1
2
3 1 McArthur Basin, Northern Territory, Australie. *Economic Geology*, **101**, 1189-
4 1209.
5 2
6 3 Rawlings DJ (1999) Stratigraphic resolution of a multiphase intracratonic basin
7 system: the Mc Arthur Basin, northern Australia. *Australian Journal of Earth*
8 *Sciences*, **46**, 703-723.
9 4
10 5
11 6 Richard A (2009) Circulation de saumures à la discordance socle/couverture
12 sédimentaire et formation des concentrations uranifères protérozoïques (Bassin
13 de l'Athabasca, Canada). Unpub. Thesis, Nancy Université, 234 p.
14 7
15 8
16 9 Richard A, Cathelineau M, Boiron MC, Cuney M, Banks DA, France-Lanord C, Pettke
17 T (2009) Origin of U-mineralizing brines in the Athabasca basin, Canada.
18 Goldschmidt conference, Davos, 172, A1098.
19 10
20 11
21 12 Richard A, Pettke T, Cathelineau M, Boiron MC, Mercadier J, Cuney M, Derome D
22 (2010) Mixing of U-bearing brines at Mc Arthur River U deposit, Canada: A LA-
23 ICPMS investigation of fluid inclusions. *Terra Nova*, accepted.
24 13
25 14
26 15 Rousset D, Bayer R, Guillon D, Edel JB (1993) Structure of the southern Rhine
27 graben from gravity and reflection seismic data. (ECORS - DEKORP program).
28 *Tectonophysics*, **221**, 135-153.
29 16
30 17
31 18 Rouvier H, Henry B, Macquar JC, Leach D, Le Goff M, Thieberoz J, Lewchuk T
32 (2001) Réaimantation régionale éocène, migration de fluides et minéralisations
33 sur la bordure cévenole (France). *Bulletin de la Société géologique de France*,
34 **172**, 503-516.
35 19
36 20
37 21 Russel MJ (1978) Downward excavating hydrothermal cells and Irish-type ore
38 deposits : Importance of an understanding thick Caledonian prism. Transactions
39 of the Institution of Mining and Metallurgy. 87B, 161-171.
40 22
41 23
42 24 Sanchez V, Vindel E, Martin-Crespo M, Corbella M Cardellach E, Banks DA (2009)
43 Sources and composition of fluids associated with fluorite deposits of Asturias
44 (N Spain). *Geofluids*, **9**, 338-355.
45 25
46 26
47 27 Sanchez V, Cardellach E, Corbella M, Vindel E, Martin-Crespo M, Boyce AJ (2010)
48 Variability in fluid sources in the fluorite deposits from Asturias (N Spain) :
49 Further evidences from REE, radiogenic (Sr, Sm, Nd) and stable (S, C, O)
50 isotope data. *Ore Geology Reviews*, doi : 10.1016/j.oregeorev.2009.12001.
51 28
52 29
53 30 Sausse J (2002) Hydromechanical properties and alteration of natural fracture
54 surface in the Soultz granite (Bas Rhin, France). *Tectonophysics*, **348**, 169-185.
55 31
56 32
57 33
58
59
60

- 1
2
3 1 Sausse J, Fourar M, Genter A (2006) Permeability and alteration within the Soultz
4 granite inferred from geophysical and flow log analysis. *Geothermics*, **35**, 544-
5 560.
6
7
8 4 Schuler C, Steiger RH (1978) On the genesis of feldspar megacryst in granites: Rb/Sr
9 isotopic study. In: *4th Conference of Geochronology Isotope Geology* (Ed
10 Zartmann RE), 386-387.
11
12 7 Shaw A, Downes H, Thirlwall MF (1993) The quartz diorites of Limousin: elemental
13 and isotopic evidence for Devonian-Carboniferous subduction in the Hercynian
14 belt of the French Massif Central. *Chemical Geology*, **107**, 1-18.
15
16 10 Sims PK, Stein HJ (2003) Tectonic evolution of the Proterozoic Colorado province,
17 Southern Rocky Mountains: a summary and appraisal. *Rocky Mountain*
18 *Geology*, **38**, 183-204.
19
20 13 Smith M.P, Savary V, Yardley BWD, Valley JW, Royer JJ, Dubois M (1998) The
21 evolution of the deep flow regime at Soultz - sous - Forêts, Rhine graben,
22 eastern France: Evidence from a composite quartz vein. *Journal of Geophysical*
23 *Research*, **103**, B11, 27223-27237.
24
25 17 Stille P, Gauthier-Lafaye F, Bros R (1993) The Neodymium isotope system as a tool
26 for petroleum exploration. *Geochimica Cosmochimica Acta*, **57**, 4521-4525.
27
28 19 Sweet IP, Brakel AT Carson L (1999) The Kombolgie Subgroup-a new look at an old
29 "formation". *AGSO Research Newsletter*, **30**, 26-28.
30
31 21 Todt W (1976) Zirkon U/Pb alter des Malsburger granits vom Süd Schwarzwald.
32 *N.Jb.Miner. Mh*, **12**, 532-544.
33
34 23 Verma S, Santoyo E, (1997) New improved equations for Na/K, Na/Li and SiO₂
geothermometers by outlier detection and rejection. *Journal of Volcanic and*
Geothermal Research, **79**, 9-23.
47
48 26 Wilkinson JJ, Everett CE, Boyce AJ, Gleeson SA, Rye DM (2005) Intracratonic
49 crustal seawater circulation and the genesis of subseafloor zinc-lead
50 mineralization in the Irish orefield. *Geology*, **33**, 805 – 808.
51
52 29 Wilkinson JJ, Stoffell B, Wilkinson CC, Jeffries TE, Appold MS (2009) Anomalously
53 metal-rich fluids form hydrothermal ore deposits. *Science*, **323**, 764-767.
54
55 31 Yardley BWD (2005) Metal concentrations in crustal fluids and their relationship to
56 ore formation. *Economic Geology*, **100**, 613-632.
57
58 33 Yardley BWD, Banks DA, Barnicoat AC (2000) The chemistry of crustal brines:
59 tracking their origins. In: *Hydrothermal iron oxide copper gold and related*
60

- 1
2
3 1 deposits, a global perspective. Porter T.M. Eds, Australian Mineral Foundation,
4 61-70.
5 2
6 3 Ziserman A (1980) Le gisement de Chaillac (Indre): la barytine des Redoutières, la
7 fluorine du Rossignol. Association d'un gîte stratiforme de couverture et d'un
8 gîte filonien du socle . 26° CGI, Gisements français, Fascicule E3.
9 4
10 5
11
12
13
14
15
16
17
18
19
20
21
22
23
24
25
26
27
28
29
30
31
32
33
34
35
36
37
38
39
40
41
42
43
44
45
46
47
48
49
50
51
52
53
54
55
56
57
58
59
60

Draft Copy

Figure captions

Fig. 1: Model of fluid migration around uranium deposit in Mid-Proterozoic series with brine penetration in the basement due to both gravity driven process and thermal convection (example of the Athabasca basin).

Fig. 2: Fluid migration around the Oklo deposit showing the penetration of recharge fluids from relief zones west of the Franceville rift zone and the mixing of brines and oil with recharge fluids along the fault zones at the edge of the basin, and near the contact between the FA/FB sedimentary formations (modified from Gauthier-Lafaye, 1986).

Fig. 3: Schematic model of the fluid circulation in the north-western part of the French Massif Central at the unconformity of the basement and sedimentary cover interface, showing the upward brine migration below the Toarcian rock and mixing in fault zones (based on data from Boiron *et al.* 2002).

Fig. 4: Schematic model of the fluid circulation in the Maestrat Pb – Zn deposit (Spain) (modified from Grandia *et al.* 2003a).

Fig. 5: Fluid migration in Silesian Pb – Zn deposits (Poland) (modified from Heijlen *et al.* 2003).

Fig. 6: Model of fluid circulation occurring in the Irish carbonate hosted Pb-Zn deposits (modified from Wilkinson *et al.* 2005).

Fig 7: Model of fluid circulation in the basement of the Rhine graben showing deep penetration of sedimentary brines down to 5 km depth and fluid mixing with recharge meteoric water.

Fig. 8: Tm ice versus Th diagram applied to aqueous fluid inclusions from two unconformity related uranium deposits (Kombolgie basin, Australia and Oklo, Gabon) and two examples of fluid circulation related to extension tectonics (Northwestern French Massif Central and Rhine Graben).

Fig. 9: Overview of the T_m ice - T_h relationships for several examples of mixing trends between two or three fluid end-members. i) full circle: Ca- (Mg-K) brines, ii) half circle: Na-(Ca-Mg) brines, empty circle: dilute hot recharge fluids.

Fig. 10: Na/K versus Na/Ca molar ratio diagram applied to fluid inclusion chemical data. 1 - Na-rich brines and 2 - Ca-rich brines, LA-ICPMS data, Mc Arthur River, Athabasca basin (Richard 2009) 3 - Aligator River, crush leach data, (Derome *et al.* 2005), 4 - Oklo, (Mathieu *et al.* 2000), 5 - Poitou High, crush leach data, (Boiron *et al.* 2002), 6 - Oil field brines (Carpenter *et al.* 1974, Karakha *et al.* 1987), 7 - Deep basin brines (Fisher & Kreitler, 1987), 8 - Silvermines Pb-Zn deposits, crush leach data, (Wilkinson *et al.* 2005), 9 - Silesia Pb-Zn deposits, crush leach data, (Heijlen *et al.* 2003), 10 - Fluorite deposits in Asturias, LA-ICPMS data, (Sanchez *et al.* 2009), 11 - Fluorite deposits NE Spain, LA-ICPMS data, (Piqué *et al.* 2008). Full circle: KTB fluids, (Möller *et al.* 2005), full triangle, Rhine graben fluids (Pauwels *et al.* 1993) full diamond: seawater, empty diamond: seawater having passed halite saturation, data from Fontes & Matray (1993). H: halite, B: bischofite. Arrows indicate the main trends related to water-rock interactions. Pl: plagioclase, Kf: K-feldspar.

Fig. 11: Cl/Br (molar ratio) versus Cl content of fluid compositions determined by crush leach analysis. Full line: seawater evaporation trend from Fontes and Matray (1993). SW: seawater, MW: meteoric water, G: gypsum, H: halite, E: Epsomite, B: Bischofite. The two dashed lines show the composition of a mixed fluid between either seawater or meteoric water with seawater having reached epsomite saturation. In the diagram for U deposits from Kombolgie basin, In the upper left diagram, the grey box shows the location of the data obtained for the Mc Arthur and Rabbit Lake uranium deposit (Athabasca basin, Richard 2009). In the lower left diagram (Soultz), the open circles refer to the data obtained on formation waters from Triassic to Oligocene series by Pauwells *et al.* (1993).

Fig. 12: Cl/Br ratios obtained by crush leach analysis for the different reported occurrences.

1
2
3 1 1 - Mc Arthur River, Athabasca basin (Richard 2009) 2- Aligator River, (Derome *et al.*
4 2005), 3- Oklo, (Mathieu *et al.* 2000), 4- Silver Mines Pb-Zn deposits, (Wilkinson *et*
5 2005), 5 - Silesia Pb-Zn deposits, (Heijlen *et al.* 2003), 6- Maestrat basin Pb-Zn
6 deposit, Spain, (Grandia *et al.* 2003a), 7 – Cantabrian Pb-Zn deposits, Spain
7 (Grandia *et al.* 2003b), the dash line shows high Cl/Br ratio related to the presence of
8 salt dome, 8 – Poitou High Pb-Zn-F deposits, (Boiron *et al.* 2002), 9 – Fluorite
9 deposits in Asturias, (Sanchez *et al.* 2009), 10 - Fluorite deposits, NE Spain, (Piqué
10 *et al.* 2008), 11- Soultz, unpublished data.
11
12 Seawater evaporation trend from Fontes & Matray (1993), SW: seawater, H_b: halite
13 beginning, H_{end} : halite end, E: epsomite.
14
15
16
17
18
19
20
21
22

23 12 Fig. 13: General conceptual model for the genesis of basement and carbonated
24 hosted deposits near the basin / basement unconformity.
25
26
27
28
29
30
31
32
33
34
35
36
37
38
39
40
41
42
43
44
45
46
47
48
49
50
51
52
53
54
55
56
57
58
59
60

1
2
3
4
5
6
7
8
9
10
11
12
13
14
15
16
17
18
19
20
21
22
23
24
25
26
27
28
29
30
31
32
33
34
35
36
37
38
39
40
41
42
43
44
45
46
47
48
49
50
51
52
53
54
55
56
57
58
59
60

2 **Table captions**

4 Table 1: Geological setting, geodynamic context and ages of the host formations and
5 mineralisations in the considered areas.

6 1 - Alexandrov *et al.* (2001), 2- Schuler & Steiger (1978), 3 – Todt (1976), 4- Bertrand
7 *et al.* (2001), 5 – Enrique *et al.* (1999), 6- Grandia *et al.* (2003a), 7- Pique *et al.*
8 (2008), 8 - Sanchez *et al.* (2010), 9 - Heijlen *et al.* (2003), 10 - Ludwig *et al.* (1987),
9 11- Maas (1989), 12 – Cummings & Krstic (1992), 13 – Alexandre *et al.* (2009), 14-
10 Stille *et al.* (1993), 15 - Bonhomme *et al.* (1982), 16- Gancarz (1978), 17 - Holliger
11 (1988)

13 Table 2: Summary of paleofluids data available on the different areas. Tm ice:
14 melting temperature of ice, Th: homogenisation temperature

16 Table 3: Main characteristics of fluid circulation in the different areas.

17 X indicates the presence of the considered process, XX indicates that the process is
18 relatively important and (X) that the process is suspected.

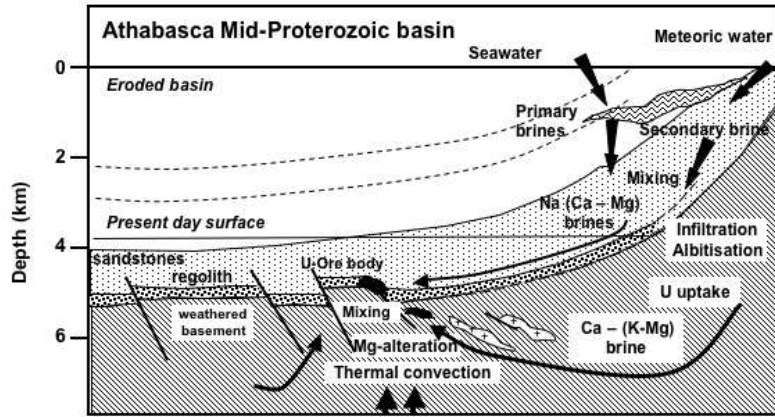


Fig 1 Boiron et al.

1
2
3
4
5
6
7
8
9
10
11
12
13
14
15
16
17
18
19
20
21
22
23
24
25
26
27
28
29
30
31
32
33
34
35
36
37
38
39
40
41
42
43
44
45
46
47
48
49
50
51
52
53
54
55
56
57
58
59
60

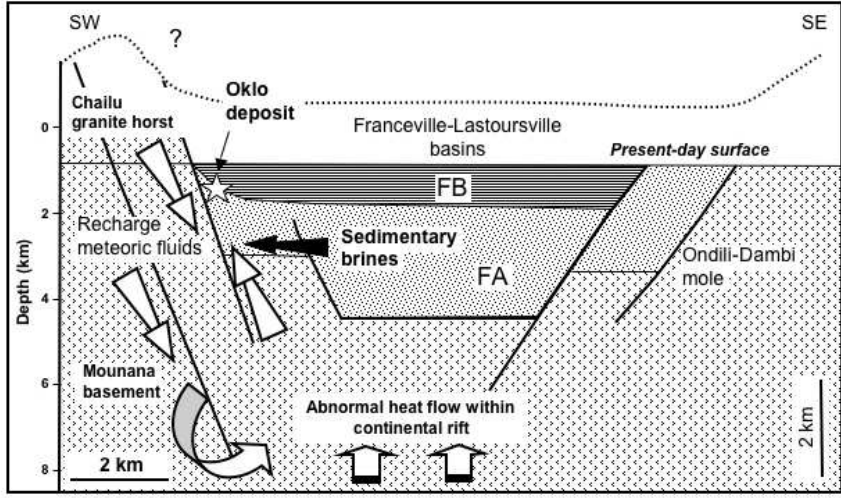


Fig 2 Boiron et al.

copy

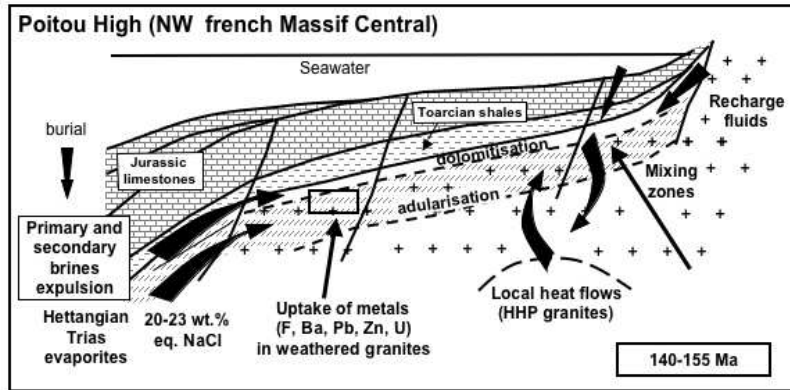


Fig 3 Boiron et al.

1
2
3
4
5
6
7
8
9
10
11
12
13
14
15
16
17
18
19
20
21
22
23
24
25
26
27
28
29
30
31
32
33
34
35
36
37
38
39
40
41
42
43
44
45
46
47
48
49
50
51
52
53
54
55
56
57
58
59
60

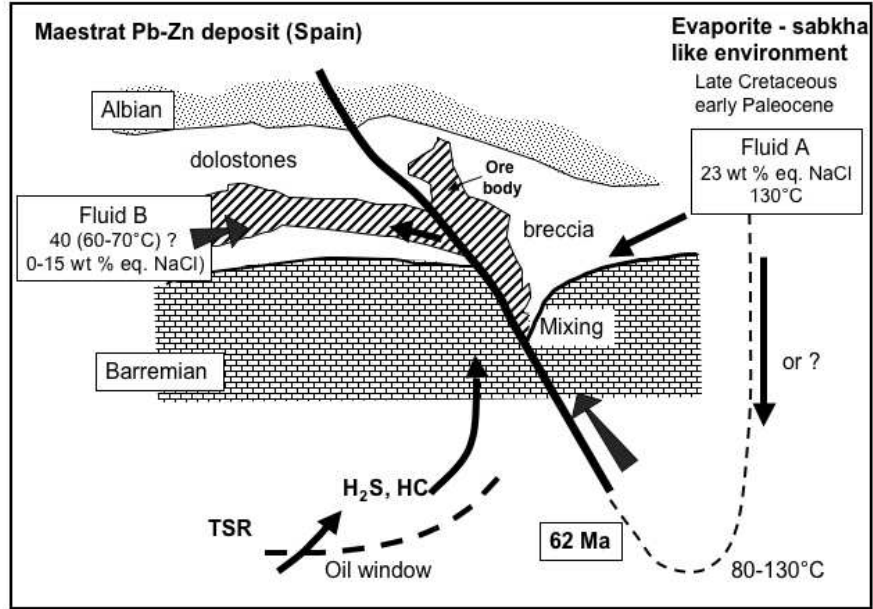


Fig 4 Boiron et al.

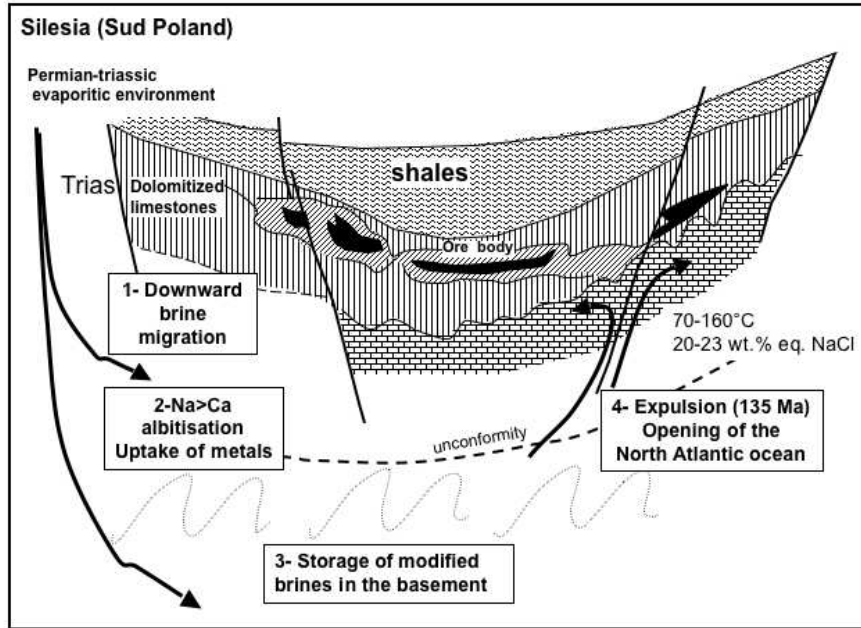


Fig 5 Boiron et al.

1
2
3
4
5
6
7
8
9
10
11
12
13
14
15
16
17
18
19
20
21
22
23
24
25
26
27
28
29
30
31
32
33
34
35
36
37
38
39
40
41
42
43
44
45
46
47
48
49
50
51
52
53
54
55
56
57
58
59
60

copy

1
2
3
4
5
6
7
8
9
10
11
12
13
14
15
16
17
18
19
20
21
22
23
24
25
26
27
28
29
30
31
32
33
34
35
36
37
38
39
40
41
42
43
44
45
46
47
48
49
50
51
52
53
54
55
56
57
58
59
60

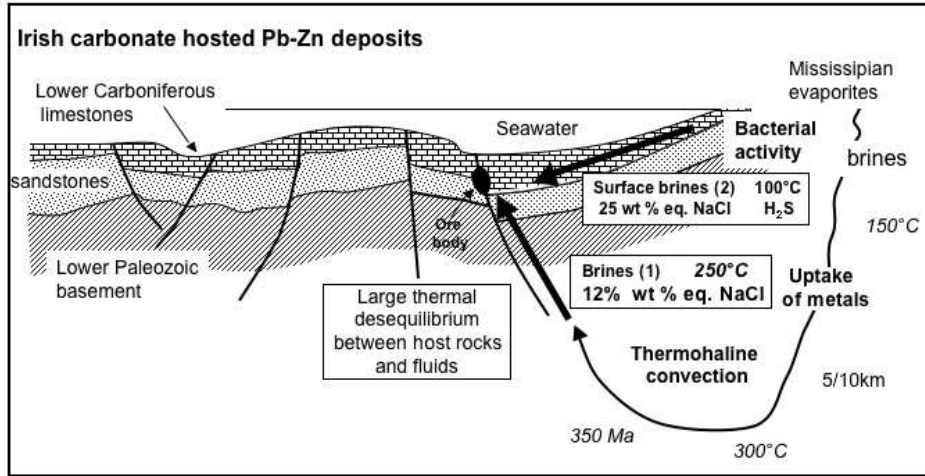


Fig 6 Boiron et al.

1
2
3
4
5
6
7
8
9
10
11
12
13
14
15
16
17
18
19
20
21
22
23
24
25
26
27
28
29
30
31
32
33
34
35
36
37
38
39
40
41
42
43
44
45
46
47
48
49
50
51
52
53
54
55
56
57
58
59
60

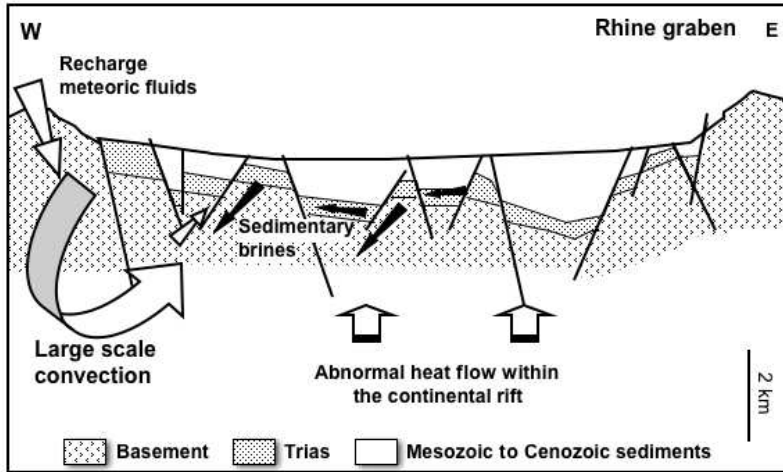


Fig 7 Boiron et al.

1
2
3
4
5
6
7
8
9
10
11
12
13
14
15
16
17
18
19
20
21
22
23
24
25
26
27
28
29
30
31
32
33
34
35
36
37
38
39
40
41
42
43
44
45
46
47
48
49
50
51
52
53
54
55
56
57
58
59
60

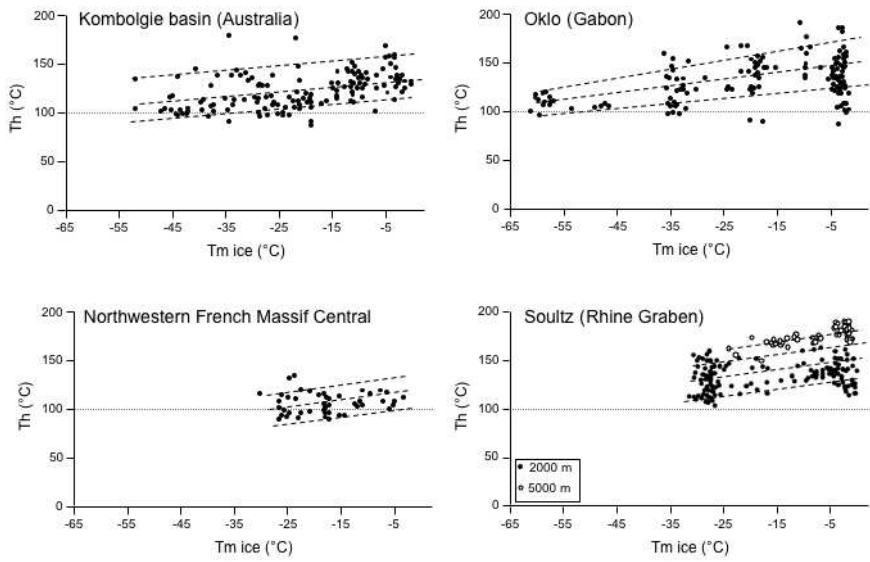


Fig. 8 Boiron et al

Copy

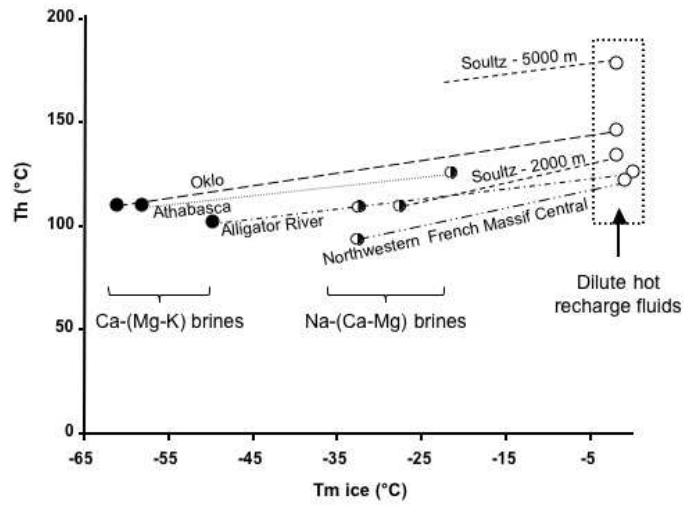


Fig. 9 Boiron et al

1
2
3
4
5
6
7
8
9
10
11
12
13
14
15
16
17
18
19
20
21
22
23
24
25
26
27
28
29
30
31
32
33
34
35
36
37
38
39
40
41
42
43
44
45
46
47
48
49
50
51
52
53
54
55
56
57
58
59
60

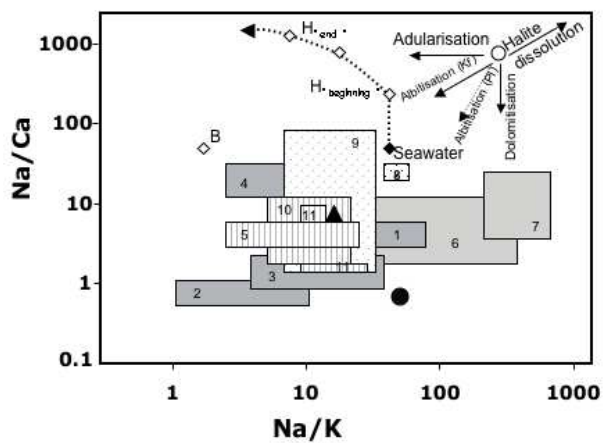


Fig. 10 Boiron et al

copy

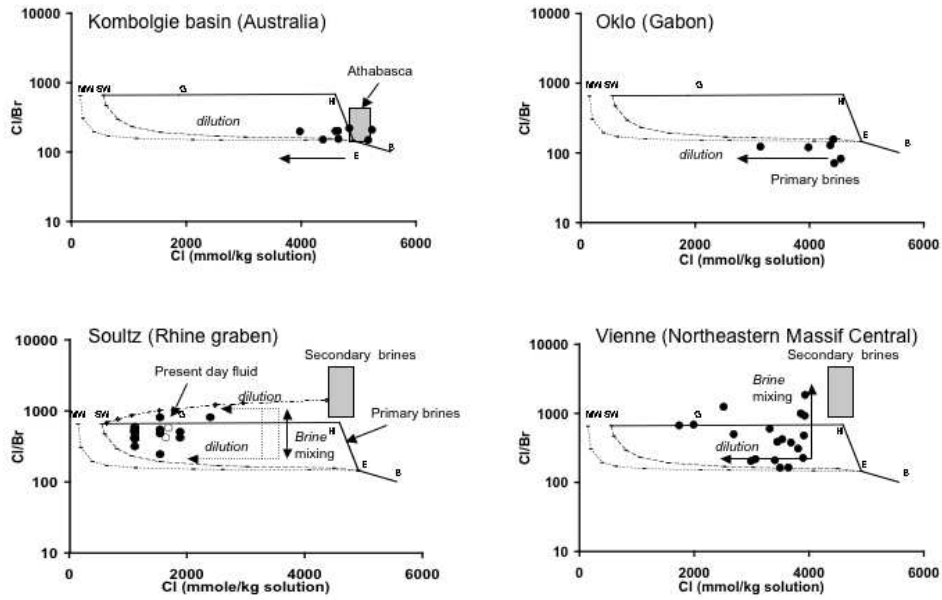


Fig. 11 Boiron et al

copy

1
2
3
4
5
6
7
8
9
10
11
12
13
14
15
16
17
18
19
20
21
22
23
24
25
26
27
28
29
30
31
32
33
34
35
36
37
38
39
40
41
42
43
44
45
46
47
48
49
50
51
52
53
54
55
56
57
58
59
60

1
2
3
4
5
6
7
8
9
10
11
12
13
14
15
16
17
18
19
20
21
22
23
24
25
26
27
28
29
30
31
32
33
34
35
36
37
38
39
40
41
42
43
44
45
46
47
48
49
50
51
52
53
54
55
56
57
58
59
60

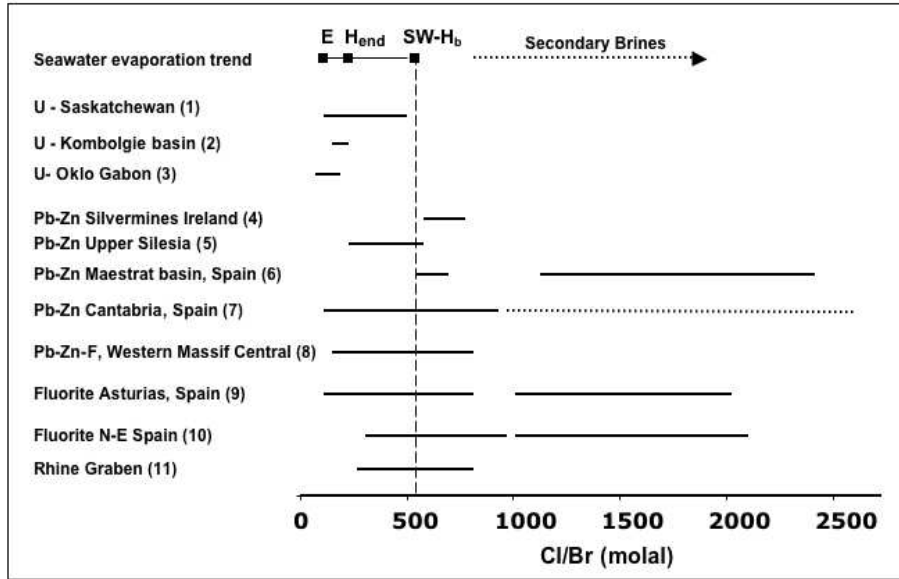


Fig. 12 Boiron et al

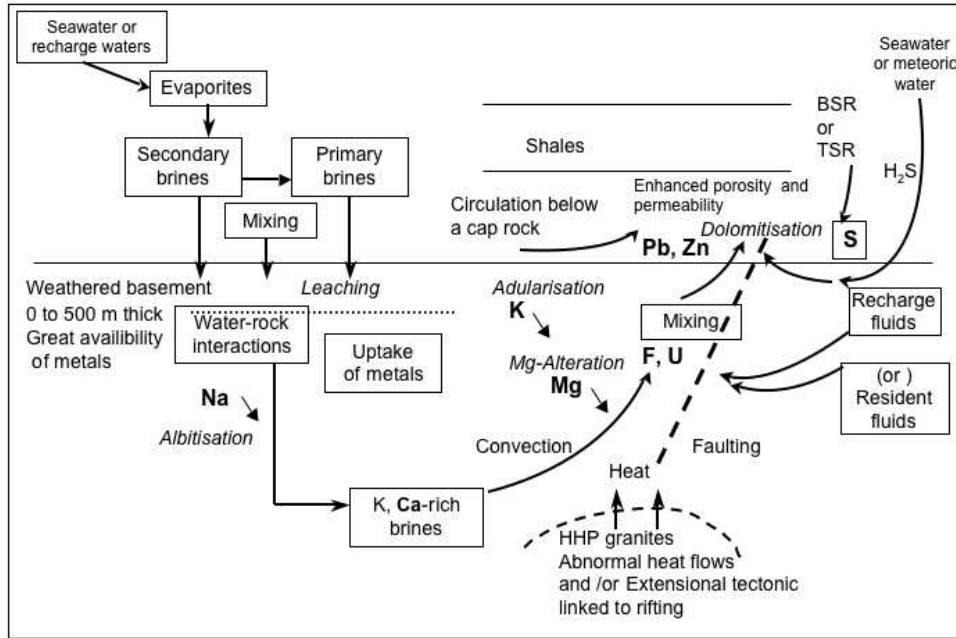


Fig 13 Boiron et al

	Location	Sedimentary cover	Basement	Age of evaporite	Ages of mineralisation (Ma)	Time gap between sedimentation and fluid movement	Geodynamic context
F-Ba	Rhine Graben Soultz sous Forêts	Eocene to Oligocene marls and clays Triassic sediments	Hercynian monzogranites (331±9 Ma) (1)	Keuper Trias	20 to present day	180 to 200 Ma	Oceanic extension - Jurassic Continental extension - Tertiary
Pb-Zn-F-Ba	Schwarzwald district Germany	Triassic sandstones Marine carbonate rich sediments	Albtal and Malsburg granites 326±2 Ma and 328±6 Ma (2,3)	Keuper Trias	Jurassic (110-150) Tertiary	70 to >130 Ma	Oceanic extension - Jurassic Continental extension - Tertiary
Pb-Zn-F-Ba	North Western French Massif Central	Marine infra-Lias to Dogger series	Hercynian tonalites to granodiorite 350 to 360 Ma (4) Peraluminous intrusions (320 Ma)	Trias at 200km Hettangian	140-155	40 to 50 Ma	Atlantic Ocean extensional tectonic
F - Ba	Albigeois	Eroded	Paleozoic basement	Trias Hettangian Continental basin	150	40 to 50 Ma	Atlantic Ocean extensional tectonic
Pb-Zn	Malines	Triassic calcareous shales silt, evaporite + Jurassic series	Lower and middle Cambrian dolomitic limestones	Trias	at less post Hettangian probably Kimeridgian	55 Ma (Trias) 340 (Cambrian)	Extensional tectonic
Pb-Zn	Maestrat basin Eastern Spain	Late Jurassic to early Cretaceous sediments	Paleozoic basement	Late Cretaceous Early Paleocene	62± 0.7 (6)	0	Slightly post-rift Gascogne gulf
F - Ba	North Eastern Spain	Triassic carbonates and evaporites Jurassic- Cretaceous limestones	Granodiorite 287 ± 2.8 Ma (5)	Trias	137 ±25 (Sm-Nd)(7)	50- 60 Ma	Extension opening atlantic ocean
F - Ba	Asturias (Spain)	Permo - Triassic series	Cambrian to Devonian basement	Permo-Trias	185 ±28 Ma (Sm-Nd) (8)	>20 Ma	Extension Atlantic Ocean opening
Pb-Zn	Upper Silesia	Trias dolomitized limestones	Carboniferous basement	Trias	135 ± 4 (9)	80 Ma	Permian grabben
Pb-Zn	Silvermines District Ireland	Lower carboniferous limestones	Low grade paleozoic metasediments	Mississippian	350 Ma	0	Local extensional rift zone or extending tectonics passive margin
U	Alligator River Australia	Kombolgie sandstones and conglomerates marine origin	Archean to early Proterozoic granite gneiss	1.7 Ga	1737 ± 20 (10) 1600 -1650 (11)	100 to 200 Ma	see discussion
U	Athabasca basin Canada	Proterozoic sandstones	Paleoproterozoic gneiss and pegmatoids	1.7 Ga	1400- 1500 (12, 13)	200 to 300 Ma	see discussion
U	Franceville basin Oklo (Gabon)	Francevillian series, Conglomerate to fine sandstones (2100 Ma) (14)	Archean K-rich plutonites 2880 to 2400 Ma (15)	in the sediment series	1960 to 2050 (16, 17)	50 to 200 Ma	continental extension

	Location	Tm ice (°C)	Th (°C)	Cl/Br (molar)	$\delta^{18}\text{O}$ fluid (‰)	δD fluid (‰)	References
F-Ba	Rhine Graben Soultz sous Forêts	2000 m : -0.2 to -31.6 5000 m : -0.1 to -24.6	2000m : 100 to 165 5000m : 150 to 184	250 to 800 *	-3 to 2	-37 to -42	Dubois et al. (1996) Smith et al. (1998) Cathelineau & Boiron (2009) Pauwels et al. (1993)
Pb-Zn-F-Ba	Schwarzwald district Germany	-0.1 to -36	80 to 200	not available	- 11.6 to -3	-10 to -60	Baatartsoqt et al. (2007)
Pb-Zn-F Ba	North Western French Massif Central	-3.8 to -30.2	80 to 130	160 to 1800	5 to 9	-19 to -50	Boiron et al. (2002)
F - Ba	Albigeois	-16.7 to -20.6	125 to 170	not available	0.1 to 3.2	-15 to -63	Munoz et al.(1999)
Pb-Zn	Malines	-10 to -16	150	not available	5.5 to 7.8	-13 to -31	Charef & Sheppard (1988)
Pb-Zn	Maestrat basin Eastern Spain	-1 to -26	70 to 130	550 to 700 1100 to 2400	0 to 3	not available	Grandia et al. (2003)
F - Ba	North Eastern Spain	-4.9 to -21.6	85 to 195 (110)	300 to 970 1000 to 2100	not available	not available	Pique et al. (2008)
F - Ba	Asturias (Spain)	-0.1 to -24.3	80 to 170	100 to 800 1000 to 8000	0.3 to 7.4	not available	Sanchez et al. (2009, 2010)
Pb-Zn	Upper Silesia	0 to -23.3	70-160	248 to 560	0 (to -3)	-10 to -30	Heijlen et al. (2003)
Pb-Zn	Silvermines District Ireland	12-18 wt %	170-240	600-770	not available	not available	Wilkinson et al. (2005)
U	Alligator River Australia	-0.3 to -52	90 to 160	150 to 220	0.9 to 3.3	not available	Derome et al. (2007)
U	Athasbaca basin Canada	-20 to -55	70 to 195	100 to 500	-3 to 6	-55 to -147	Richard (2009)
U	Franceville basin Oklo (Gabon)	-1.3 to -63	90 to 175	70 to 160	-6 to 0	not available	Mathieu et al. (2000) Mathieu (1999)

	Location	Fluid origin		Fluid recharge		Mixing	Fluid in the basement	Water-rock interaction	Main cause of metal deposition
		Primary brine	Secondary brine	Hot fluid	Cold fluid				
F-Ba	Rhine Graben Soulz sous Forêts	X	Probable	hot dilute fluid 170°C at 2000m 200°C at 5000m		X	> 5km	Illitisation	Dilution
Pb-Zn-F-Ba	Schwarzwald district Germany		deep aquifer at 300 - 350°C		resident fluid	X	7 -8 km	Illitisation	Mixing dilution
Pb-Zn-F-Ba	North Western French Massif Central	X	X	dilute in some places		X	> 1km	Adularisation (basement) Dolomitisation (infra-Lias)	Dilution Cooling
F - Ba	Albigeois		X				a few km	Silicification preceeding Fluorite deposition	Cooling
Pb-Zn	Malines		Connate waters but Triassic evaporites		resident fluid	X	X	Dolomitisation	Dilution Cooling
Pb-Zn	Maestrat basin Eastern Spain	X	X		resident fluid	X		Dolomitisation	Mixing of 2 brines
F - Ba	North Eastern Spain	X	X			X (dilution)	XX		Dilution at constant temperature
F - Ba	Asturias (Spain)	X	X		resident fluid	X	XX	Dolomitisation Silicification	Mixing with less saline surficial derived fluid present in sediments
Pb-Zn	Upper Silesia	X				X (Dolomite)	deep penetration	Dolomitisation Albitisation (basement)	Mixing Cooling
Pb-Zn	Silvermines District Ireland	deep circulating brines		cooler Ca - brine			XX	Dolomitisation in limestones	Cooling, mixing of 2 brines including a S-rich brine
U	Alligator River Australia	X	(X)	ascending hot dilute fluid		X	XX	Chlorite	Dilution
U	Athasbaca basin Canada	X	(X)	Ca- brine		X	> 1 km	Sudoite - illite (quartz dissolution)	Mixing (cooling)
U	Franceville basin Oklo (Gabon)	X	(X)	hot dilute fluid		X	X recharge	chlorite	dilution